

NASA-TM-84330 19830013888

Augmentation of Fighter Aircraft Performance by Spanwise Blowing Over the Wing Leading Edge

Arnan Seginer and Meir Salomon

March 1983

LIBRARY COPY

APR 11 1983

LANGLEY RESEARCH CENTER
LIBRARY, NASA
HAMPTON, VIRGINIA



National Aeronautics and
Space Administration

Augmentation of Fighter Aircraft Performance by Spanwise Blowing Over the Wing Leading Edge

Arnan Seginer, Ames Research Center, Moffett Field, California
Meir Salomon, SAL Engineering, Haifa, Israel



National Aeronautics and
Space Administration

Ames Research Center
Moffett Field, California 94035

N83-22159 #

AUGMENTATION OF FIGHTER-AIRCRAFT PERFORMANCE BY SPANWISE BLOWING OVER THE WING LEADING EDGE

Arnan Seginer
NASA Ames Research Center
Moffett Field, California 94035, U.S.A.

and

Meir Salomon
SAL Engineering
Haifa, Israel

SUMMARY

Spanwise blowing over the wing and canard of a 1:35 model of a close-coupled-canard fighter-airplane configuration (similar to the Kfir-C2) was investigated experimentally in low-speed flow. Tests were conducted at airspeeds of 30 m/sec (Reynolds number of 1.8×10^5 based on mean aerodynamic chord) with angle-of-attack sweeps from -8° to 60° , and yaw-angle sweeps from -8° to 36° at fixed angles of attack 0° , 10° , 20° , 25° , 30° , and 35° . Significant improvement in lift-curve slope, maximum lift, drag polar and lateral/directional stability was found, enlarging the flight envelope beyond its previous low-speed/maximum-lift limit. In spite of the highly swept (60°) leading edge, the efficiency of the lift augmentation by blowing was relatively high and was found to increase with increasing blowing momentum on the close-coupled-canard configuration. Interesting possibilities of obtaining much higher efficiencies with swirling jets were indicated.

LIST OF SYMBOLS

C_D	drag coefficient, including jet thrust
C_L	lift coefficient, including jet thrust
$C_{L_{max}}$	maximum-lift coefficient, including jet thrust
ΔC_L	lift increment due to blowing, including jet thrust
C_N	yawing-moment coefficient, including jet thrust
C_R	rolling-moment coefficient, including jet thrust
C_Y	side-force coefficient, including jet thrust
C_μ	jet-momentum coefficient, equal to the product of the jet mass flux and its exit velocity normalized by the free-flow dynamic pressure and the wing-planform area
Re	Reynolds number
α	angle of attack
ψ	yaw angle

Subscripts

B	relative to the body frame of reference
c	on the canard
T	net aerodynamic coefficient corrected for jet thrust
w	on the wing

1. INTRODUCTION

One of the persistent goals in the design of advanced tactical fighter aircraft has been the generation of additional usable lift. It is required for improved maneuverability (this is also true for the new generation, highly maneuverable air-to-air missiles) and for good low-speed performance in takeoff and landing. Since the limits of conventional linear-lift have been reached, current modern designs use nonlinear, or vortex lift, which is characteristic of slender wings and of moderately swept wings with sharp leading edges. The leading-edge-vortex phenomenon has been understood for many years (e.g., Ref. 1). At moderate to high angles of attack the flow separates from the leading edge. The favorable spanwise pressure gradient causes the separating vortex sheet to reattach behind the leading edge and to roll up into a steady vortex over the leading edge (Fig. 1). The high velocities and low pressures induced on the wing under the vortex produce the additional lift. Polhamus, in his well-known Suction-Analogy (Ref. 2), estimated the maximum lift that can be obtained in this way. The influence of the vorticity, shed from the leading edge, on the whole flow field and on the aerodynamic characteristics of an aircraft or missile configuration can be computed by a nonlinear vortex-lattice method (Ref. 3).

The use of vortex lift is limited by vortex bursting or breakdown, which is characterized by a sudden expansion of the vortex about a rapidly decelerating core, with subsequent vortex disintegration and loss

of the orderly vortical flow. As the angle of attack is increased, the point of vortex breakdown moves upstream, causing loss of lift and, finally, stall (Ref. 4).

While leading-edge vortices on slender highly swept wings are stable at moderate to high angles of attack, moderately swept wings that are in common use on fighter aircraft suffer from vortex breakdown at low angles of attack (e.g., Fig. 3 of Ref. 5), or sometimes do not produce leading-edge vortices at all (Ref. 6). Consequently, Kuchemann (Ref. 7) suggested a compromise between the contradictory requirements of fighter wings by combining coiled vortex sheets originating from the inboard parts of the wing with conventional attached flow over its outboard parts. This led to a hybrid wing design including concave double-delta wings, straked wings, or close-coupled-canard configurations (Ref. 8). In these designs a vortex emanating from the inboard elements (slender delta, strakes, or canard) produces a leading-edge vortex on the moderately swept outer part of the wing or stabilizes an existing one. These devices are essential for the nonlinear lift of moderately swept wings (Ref. 6), and also work in delaying the vortex breakdown of highly swept wings to still higher angles of attack (e.g., the Swedish Viggen aircraft, Ref. 9, or the Israeli Kfir-C2 aircraft).

Although much has still to be learned about the basic mechanism of the vortex breakdown (Ref. 10), Cornish's description of the fluid-mechanic processes involved (Ref. 11) enabled him to apply vortex control in subsonic flow by blowing a high-velocity jet down its core. There is still some disagreement about why and how this method works. Cornish thought that the low-speed, highly vortical core was removed through entrainment by the high-speed jet. Dixon's observations (Ref. 12) indicated that the jet and the vortex did not mix until the jet had expended most of its energy. These observations were strengthened by later experiments with hot jets on large-scale vectored-engine-over-wing (VEO-Wing) STOL configurations (Refs. 13-15). Dixon's contention was that the jet acted as a barrier to the downstream motion of the leading-edge vortex and that vortex control was a function of the spanwise entrainment of the free-stream flow.

In spite of the disagreement concerning the nature of the phenomenon, the feasibility and potential benefits of spanwise-blowing (SWB) in low-speed flow were proven by the results of many experimental programs. Dixon pioneered the SWB with his flat-plate experiments (Ref. 16) and was closely followed by Cornish's SWB over a flap (Ref. 11) and Poisson-Quinton's SWB over wings (Ref. 17). The investigation developed further by testing many wing planforms and configurations (Refs. 5, 6, 8, 18, 19), and some research aircraft configurations (Refs. 8, 13, 14, 15, 20, 21). All these investigations (and many more not mentioned here) concluded that SWB generates significant lift increments and improves the drag polars at high angles of attack, with no loss (and in some cases a slight improvement) in longitudinal static stability, and usually with a significant improvement in lateral/directional stability and a delay in the departure conditions (e.g., Ref. 8). Comparisons with other high-lift devices have led to the conclusion that SWB is more effective at high angles of attack (e.g., Refs. 5, 8) and may be an alternative to mechanical flaps or strakes.

The efficiency of SWB is also in question. It is addressed in most of the investigations as the ratio, $\Delta C_L / C_u$, between the lift-coefficient increment (ΔC_L) and the thrust coefficient of the spanwise jet (or jet-momentum coefficient, C_u , which is the jet contribution to the lift when vectored vertically downwards). This ratio (rather than the ratio of the negative drag increment at a given α to the jet-momentum coefficient) is used because the main aim is to increase $C_{L_{max}}$. This efficiency is higher than 1.0 at angles of attack that are typically higher than 10° . The highest efficiencies are reported at the lowest blowing rates (Ref. 19) because of the small C_u in the denominator. As the blowing rate is increased, the efficiency decreases because of the diminishing lift increments (Ref. 8). The goal of the highest possible maximum lift ($C_{L_{max}}$) would therefore mean a low-efficiency, high blowing rate. Furthermore, the evaluation of SWB potential improvements in overall aircraft performance should also account for the loss in thrust from bleeding off engine air for the SWB. Several investigators have subtracted the thrust of the jet from the engine thrust and have come up with very promising results. Campbell (Ref. 19) concluded that SWB increases the specific excess power at load factors above 1.0 and allows higher load factors to be attained before reaching the lift limit. Dixon, Theisen, and Scruggs (Ref. 22) estimated that the A-7 Corsair II aircraft could substitute SWB for all of its high-lift devices at a cost of only 15% of its thrust. Staudacher et al. (Ref. 8) were also optimistic for the low-speed region, where the flight envelope was limited by the attainable maximum lift (that could be improved by SWB) while excess thrust was available. Erickson (Ref. 23) was less optimistic when he found a 27% reduction in thrust of the F-5E at the relatively low blowing rate of 0.012, and a corresponding reduction in specific excess power available for maneuvering. One should, however, heed Erickson's remarks that SWB may be practical when used with new and suitable engines. An example of such innovative thought is the VEO-Wing concept (Refs. 13-15), where up to 16% of the engine exhaust was diverted to the SWB system.

Erickson's investigation of an existing fighter configuration (Ref. 23) is of particular interest because it provides information about the effects of SWB on its overall high-angle-of-attack aerodynamic characteristics. This is an area of ongoing interest, as can be evidenced by the NASA/DFRC-LaRC F-4C flight-test program. Therefore, for the present investigation it was decided to test existing fighter-airplane configurations at the Technion, Israel Institute of Technology (IIT). The aircraft chosen for this test was the basic low delta-wing airframe of the Dassault Mirage-IIIC that closely resembled the IAI Kfir-C1, and when equipped with a canard resembled also the configuration of the IAI Kfir-C2.

Whereas most of the configurations tested in the previously discussed references had moderately swept wings, this configuration had a 60° swept delta wing. The highly swept wing was chosen for obvious practical reasons, although it was known (Refs. 18, 19) that SWB is more efficient on wings of lower sweep; highly swept leading edges generate a sizable amount of natural vortex lift that usually could not be increased by SWB. Blowing only increased the maximum lift. Lift augmentation throughout the angle-of-attack envelope that was measured in the present investigation was, therefore, unexpected and the investigation concentrated on delaying the vortex breakdown and on increasing the maximum lift. Because this aircraft (like many others) was limited in high-lift maneuvers by lateral/directional stability and control considerations rather than by stall, special attention had to be paid to its stall-departure characteristics. The first stage of the investigation was conducted in a low-speed wind tunnel, and it is assumed that the low-speed data presented here are indicative of lift and drag augmentation at speeds up to the

critical Mach number (Ref. 20). Furthermore, at the low-speed end of the flight envelope aircraft are usually limited by their maximum lift, while they still have ample excess power. It is, therefore, in this speed regime that the spanwise blowing can most effectively improve maneuverability. Improving maneuverability in the transonic speed range would also be desirable, but vortex stabilization by SWB from the fuselage would require impractical blowing rates (Ref. 8). Transonic performance can be improved by local blowing from the wing (Ref. 24) but that is a result of shock-induced-separation control rather than vortex stabilization. Therefore, transonic testing would have to be done at a later stage.

In addition, the investigation includes a comparison of SWB with the effects of the canard, asymmetric blowing (to study the effects of a malfunctioning blowing system), and blowing of swirling jets (to evaluate the various theories on the SWB mechanism).

2. EXPERIMENTAL APPARATUS AND TESTS

2.1 The Model

The model used in this study (Fig. 2) is a 1:35-scale metal-reinforced plastic replica of the aircraft with the twin inlets faired over. The model has a low delta wing with a relatively sharp leading edge that has a conical droop and is swept back 60° . The basic model (no canard) is designated as Configuration A in the following discussion. The same model can also be equipped with a canard mounted on the engine inlets at a height of 0.31 local fuselage diameter above the wing. The canard has a leading-edge sweep angle of 45° and a span of 44% of the wing span (fuselage included). The model with the canard is designated as Configuration B.

Four convergent steel nozzles were installed in the model, two on each side of the fuselage, one above the wing and one above the canard. The wing nozzles (2.3 mm in diameter) issued a jet parallel to the wing leading edge. Their location, one diameter above the wing surface and 10% of the root chord from the leading edge, was determined by preliminary tests on a larger model (not reported). The effects of the vertical position on the blowing were rather small. The axial location had a somewhat stronger influence, with the blowing becoming more effective as the nozzles were moved aft. The location used in the present experiments was the farthest aft that was consistent with the structure of the inlets of the existing aircraft. The canard nozzles had a 1.3 mm diameter and their location relative to the canard was similar to the location of the wing nozzles relative to the wing.

2.2 The Blowing System

Compressed air at pressures up to 8 atm was supplied to the model's nozzles from the laboratory's low-pressure system through flexible hoses along the model sting-support, and through stainless steel tubes inside the model. Air could be blown from any single nozzle when asymmetric blowing was investigated; or from all four nozzles simultaneously, or separately from the wing or canard nozzles only. Swirling jets were obtained from the same nozzles by inserting drill bits because good swirl nozzles could not be manufactured due to their small size. Swirl direction was controlled by using right- or left-hand bits. The inserts reduced the nozzle cross-section area by about 75%. It is not known how much swirl was actually imparted to the jets by this method.

2.3 Wind Tunnel and Instrumentation

The tests were conducted in the $1\text{ m} \times 1\text{ m}$ (3-m long) test section of the low-speed atmospheric wind tunnel of the Aeronautical Research Center, Technion, IIT. Airspeed in all of the tests was 30 m/sec with a corresponding Reynolds number of $-1.8 \times 10^6/\text{m}$ or 1.8×10^5 , based on the mean aerodynamic chord.

The model was mounted on a six-component internal strain-gage sting balance, and the data were acquired and reduced to aerodynamic coefficients by an NEFF620/Elbit-CR 17 data-acquisition/computer system. Forces were conventionally normalized by the free-stream dynamic pressure and the wing area; moments, measured relative to a reference point at 48% of the root-chord, were normalized with the mean aerodynamic chord. The longitudinal aerodynamic coefficients were computed in the wind frame of reference whereas the lateral coefficients were computed and presented in the body frame of reference.

2.4 Force Tests

The longitudinal aerodynamic coefficients were measured at 0° yaw angle during angle-of-attack sweeps from -8° to 60° , and the lateral coefficients were measured during yaw-angle sweeps from -8° to 36° at fixed angles of attack of 0° , 10° , 20° , 25° , 30° , and 35° . Blowing stagnation pressures were 4, 6, and 8 atm for the wing and 4 and 6 atm for the canard, corresponding to jet-momentum coefficients of 0.05, 0.07, and 0.09 on the wing, and 0.016 and 0.022 on the canard. In the asymmetric-blowing tests on one wing only, the jet-momentum coefficient was 0.025, 0.035, and 0.045, and in the swirling-jet experiments it was -0.012 (for a blowing pressure of 4 atm).

Before beginning the wind-tunnel tests, all the nozzles were plugged and the air-feed and blowing systems were pressurized to ensure that the balance was not affected by stiffening of the air hoses and tubes. The nozzles were then unplugged and the direct contributions of the jets to the lift and the thrust were recorded without flow in the tunnel, later to be subtracted from the values measured with flow in the tunnel. The results presented here for Configuration A are net aerodynamic results corrected for the contributions of the jet momentum. The results for Configuration B were not corrected and the aerodynamic coefficients include the contributions from the jets; these contributions are presented so that the results with thrust removed can be calculated. The correction for the thrust contributions is the aerodynamicist's way of evaluating the net aerodynamic effects of SWB, but since the actual aircraft experiences the total lift and drag, these are shown for Configuration B. The thrust loss should also be taken into account but must be measured on the actual engine (Ref. 23). It is interesting to note that the thrust resulting from the jets was larger than the streamwise component of the jet momentum, possibly because of suction over the leading-edge droop.

2.5 Flow-Visualization Tests

Some flow-visualization tests were conducted using a helium bubble generator. Bubbles are generated by blowing a helium-air stream through a liquid detergent. The bubbles are filtered so that only the neutrally buoyant bubbles are injected into the wind tunnel through a nozzle and follow the air-flow streamlines. The bubbles reflect the light of a high-intensity spotlight and can be seen against the dark background of the black-painted model and wind-tunnel walls. Flow visualization was used to study the characteristics of the flow over the wing and the canard and to correlate them with the force measurements. An example is presented in Figs. 3 and 4 where the model is at an angle of attack of -35° . The streamlines over a section of the wing leading edge are shown in Fig. 3a without blowing ($C_{\mu} = 0$). The flow is separated from the leading edge onwards. There is no observable orderly pattern and some reversed flow can be seen. When the spanwise blowing ($C_{\mu} = 0.07$) is turned on (Fig. 3b), the flow is seen to reattach behind an orderly vortex. The vortex core is clearly defined with its breakdown occurring somewhere over the trailing edge. Figure 4a shows the flow over the canard under the same conditions without blowing. The canard does not seem to have any effect on the flow field. In fact, the local flow seems to be separated from the canard and the wing. When air is blown over the canard and the wing ($C_{\mu C} = 0.022$, $C_{\mu W} = 0.07$), a vortex is formed over the canard, and the flow over the vortex turns downward and reattaches to the wing (Fig. 4b).

3. RESULTS AND DISCUSSION

3.1 Configuration A

Symmetric blowing. The effects of blowing on the lift coefficient (corrected for the jet contribution) are shown in Fig. 5. Contrary to previous experience with wings of high sweep angles (Refs. 18, 19), blowing not only increases the maximum-lift values, but also increases the lift-curve slope. The slope increment at low angles of attack ($\alpha < 12^\circ$) was small but unmistakable and was probably due to an increased effective camber (Ref. 19). At higher angles of attack there was an appreciable increase in the slope and the maximum-lift coefficient was increased from 1.37 to 1.67. The angle of attack for maximum lift was increased by only about 1° , from 34° to 35° . An increase in the jet-momentum coefficient from $C_{\mu} = 0.05$ to $C_{\mu} = 0.07$ had a small effect, and was unjustifiable as far as efficiency was concerned.

Figure 6 presents the improvement in the drag polar after subtraction of the thrust of the jets. There was a slight decrease in the zero-lift drag, possibly because of some increase in leading-edge suction, and although the drag for any other given angle of attack was higher with blowing than without blowing, there was a significant reduction in drag for any given lift coefficient. Blowing had no effect on the longitudinal static stability except for extending the stable region (not shown) to the new $C_{L_{\max}}$ without pitchup (e.g., Refs. 8, 21, 23).

Asymmetric blowing. The effects of asymmetric blowing had to be investigated in order to assure that the control surfaces could cope with the asymmetric loads on the airframe in the case of a malfunction. The effects of blowing over the left wing only are shown in Figs. 7-10. The previous blowing coefficients of 0.05 and 0.07 were halved to 0.025 and 0.035 and the lift increments resulting from blowing were lower than with symmetric blowing, but by less than 50% (Fig. 7). Increasing the blowing pressure to 8 atm and the blowing coefficient to $C_{\mu} = 0.045$ brought the $C_{L_{\max}}$ back to the value of 1.65, almost the value achieved with $C_{\mu} = 0.07$. This gives some insight into the effects of blowing rate, and it seems that $C_{\mu} = 0.045 \div 0.05$ is the maximum needed. Interestingly, the asymmetric blowing increased the angle of attack of maximum lift to $\alpha = 38^\circ$.

Asymmetric blowing had no detrimental effects on the lift. No new effects on the drag or the pitching moment were expected or observed. On the other hand, effects on the lateral aerodynamic coefficients were expected, but the measured side force (thrust not removed) (Fig. 8) was small and probably attributable to the jet thrust. The small asymmetry of the side force was also observed without blowing and must have been the result of some model asymmetry. The sudden dip in the side force at $32^\circ < \alpha < 58^\circ$ and the sign reversal at still higher angles of attack, that are apparently the result of asymmetric separation and vortex shedding from the fuselage, were not affected by the blowing.

The trend of the uncorrected yawing moment (Fig. 9) is similar to that of the side force. The additional moment resulting from blowing is not large and can be controlled by the rudder. The effect on the corrected rolling moment was more significant (Fig. 10). Blowing over the left wing only and increasing its lift had a dramatic effect at angles of attack above 12° , when it generated a strong positive rolling moment. This continued up to $\alpha \approx 40^\circ$, when the moment was drastically reduced. The moment was not too large for the ailerons to handle; moreover, such an effect could be used for rapid roll control as an aid to the ailerons. The sudden dip in the rolling moment at $\alpha > 32^\circ$ without blowing, or at $\alpha > 36^\circ \div 40^\circ$ with blowing, is again related to the asymmetric separation on the nose.

Swirling jets. As stated before, it was Cornish's contention (Ref. 11) that the jet's function was to flow down the core of the vortex and, acting like a spanwise line sink, remove by entrainment the low-velocity high-vorticity core flow. Later experiments showed, however, that the jet and the vortex did not mix (Refs. 13-15). Dixon (Ref. 12) on the other hand, believed that the leading-edge-vortex breakdown phenomenon was a result of its helix angle becoming less than 42° , or a result of the ratio of the vortex swirl velocity to the axial velocity becoming greater than 1.12. This happened when the vortex began to turn downstream. Dixon reasoned that SWB prevented or delayed the vortex breakdown by acting as a barrier and correlated the effectiveness of SWB with its spanwise entrainment of free-stream flow. Increasing the SWB effects should therefore result from improved mixing of the jet with the free stream and would also require the longest possible spanwise reach of the jet.

Several experiments were conducted with swirling jets to test these concepts. The swirl of the jet could have several effects. Diverting some of the jet's axial momentum into its circumferential flow should shorten its active length and, therefore, reduce its effectiveness as a barrier. On the other

hand, swirl should improve its entrainment characteristics and thus its effectiveness. Also, since the vortex and jet cores have a common boundary, the jet's swirl should, according to Dixon (Ref. 12), reduce the vortex helix angle and, therefore, destabilize the vortex when they are counterrotating, and, conversely, stabilize the vortex when they are corotating.

Three different swirling-jet experiments were conducted, one with positive swirl (the jets on both wings corotating with the leading-edge vortices), a second with negative swirl (both jets counterrotating), and a third with negative swirl on the right wing and positive swirl on the left. The results were surprising. In spite of the much lower jet-momentum coefficient ($C_{\mu} = 0.012$) resulting from the reduced nozzle cross-section area, a maximum-lift coefficient of $(C_{L_{\max}})_T = 1.67$ was obtained (Fig. 11), essentially equal to the one corresponding to axial blowing with $C_{\mu} = 0.50$ (Fig. 5). The highest lift was obtained with the positive swirl, but the differences, due to swirl direction, are too small to be significant. The same is also true for the drag polar (Fig. 12).

Before drawing any conclusions from these results, one has to remember that the jet was not truly swirling, but rather made of two discrete jets emerging from the drill-bit grooves at cross angles. It is, therefore, impossible to speculate about the effects of swirl on the stability of the vortex. It can be safely assumed, however, that the two jets improved the mixing and entrainment of the free-stream flow, resulting in the dramatic increase in the lift.

Lateral aerodynamics. The side force acting on the basic model (measured in the body frame of reference) increased with yaw angle and became more nonlinear with increasing angle of attack (Fig. 13). The side force also increased with increasing jet momentum, smoothing the curves and apparently preventing local separations. The stronger effect of the SWB was on the yawing moment (Fig. 14). At the lower angles of attack ($\alpha \leq 20^\circ$) the SWB had little effect (Fig. 14a), whereas it stabilized the configuration at the higher angles of attack ($20^\circ < \alpha \leq 30^\circ$) up to high yaw angles, where without blowing it was unstable (Fig. 14b). In fact, only at $\alpha = 35^\circ$ did blowing fail to stabilize the configuration. This is a good example of an airframe that was not limited in angle of attack ($\alpha < 25^\circ$) by stall, which started only at $\alpha = 34^\circ$, but by lateral/directional instability, which was postponed by blowing to $\alpha > 30^\circ$.

3.2 Configuration B

SWB over the wing only. The canard itself increased the natural vortex lift of the wing by intensifying and stabilizing its vortex, as can be seen in the increased lift curve slope (solid curve in Fig. 15) and in the maximum lift ($C_{L_{\max}} = 1.63$). Blowing over the wing only on Configuration B further increased the vortex lift (Fig. 15, jet thrust not removed). The slope of the lift curve was increased above $\alpha = 8^\circ$ and the maximum lift was increased to 1.66 and 1.74 with blowing rates of $C_{\mu} = 0.05$ and 0.07, respectively (Fig. 15). As a result of the increase in natural vorticity, induced by the canard, the efficiency of the blowing on this configuration was lower than without a canard (Fig. 5). Without a canard $\Delta C_L/C_{\mu} = 0.28/0.05 = 5.60$ and $\Delta C_L/C_{\mu} = 0.3/0.07 = 4.29$, whereas with a canard $\Delta C_L/C_{\mu} = 0.03/0.05 = 0.60$ and $\Delta C_L/C_{\mu} = 0.11/0.07 = 1.57$. Surprisingly though, the efficiency of SWB with the higher blowing rate was in this case higher than the efficiency of SWB with the lower momentum coefficient. Obviously, if one is willing to pay the price, SWB can increase the maximum lift already obtained by high-lift devices, but at reduced efficiency. The effect of blowing over the wing only on the drag polar of Configuration B (Fig. 16) is similar to that of Configuration A, namely, an increased lift for a given drag or a reduced drag for a given lift.

SWB over both wing and canard. Blowing over both lifting surfaces increased the lift curve slope and the maximum lift more than did SWB over the wing alone (Fig. 17). With a total jet-momentum coefficient of $C_{\mu} = 0.066$ ($C_{\mu_w} = 0.05$ plus $C_{\mu_c} = 0.016$) the maximum-lift coefficient was increased to $C_{L_{\max}} = 1.78$ with an efficiency of $\Delta C_L/C_{\mu} = 0.15/0.066 = 2.27$, and with $C_{\mu} = 0.092$ ($C_{\mu_w} = 0.07$ plus $C_{\mu_c} = 0.022$) $C_{L_{\max}}$ was increased to 1.91 with an efficiency of $0.28/0.092 = 3.04$. This is also surprising, because not only was the efficiency higher with the higher jet momentum, but it was even higher than it was with blowing over the wing alone with a lower jet momentum coefficient. Figure 17 also shows the direct lift of the jets so that the pure aerodynamic lift increments resulting from blowing could be evaluated. These were $\Delta C_L = 0.11$ and 0.21, respectively, for the above-mentioned cases with thrust removed and $\Delta C_L = 0.15$ and 0.25, respectively, with thrust included.

Figure 18 shows the improvement in the drag polar without removing the thrust. The static thrust of the jets is also shown. If the thrust was subtracted from the drag, the zero-lift drag would be slightly reduced by the blowing and the lift-to-drag ratio would still be improved for all angles. With direct jet contributions included, the lift-to-drag ratio for $C_D = 1.0$ was increased from $L/D = 1.58$ to $L/D = 1.73$ and $L/D = 1.83$ for the two blowing rates presented. At the maximum lift the corresponding values of this ratio were $L/D = 1.58$ and 1.65, respectively, whereas L/D was only 1.46 without blowing.

Lateral/directional stability. With blowing over both lifting surfaces, the lateral/directional characteristics of the configuration had to be tested again. As was the case with Configuration A, SWB smoothed the curves of the side force versus yaw angle up to an angle of attack of 30° (Fig. 19). It maintained a monotonously increasing side force, apparently by preventing asymmetric-vortex breakdown and local separations and rapid shifts of the lateral center of pressure. The SWB lost its influence on the side force only at $\alpha = 35^\circ$.

The effect of blowing on the yawing moment is shown in Fig. 20. Without blowing, the configuration was gradually losing its lateral stability at lower yaw angles when the angle of attack was increased (Fig. 20a), until at $\alpha = 25^\circ$ it was too unstable for practical purposes (Fig. 20b). SWB increased the stability at the lower angles of attack (Fig. 20a) and stabilized the configuration at $\alpha = 25^\circ$ and 30° up to yaw angles of 30° and 32° . At an angle of attack of 30° , the higher blowing rate was required on both wing and canard for stabilization, but even this rate was insufficient for stabilization at $\alpha = 35^\circ$. In summary, like Configuration A, Configuration B was also limited in angle of attack by lateral/directional

instability rather than by stall. Spanwise blowing increased the flight envelope and improved performance by stabilizing the configuration and increasing the available lift.

3.3 Comparison of SWB with the Canard

Figures 21 and 22 summarize the results of this investigation. Lift and drag results, with and without the canard, are compared with and without blowing. All the results are with thrust removed. Spanwise blowing with a jet-momentum coefficient of $C_{\mu} = 0.05$ (a lower one will probably also do) gives about the same lift characteristics as the canard (Fig. 21, circles vs dashed line), both in lift-curve slope and in maximum lift, and with a much lower drag (Fig. 22). The canard increases the drag for a given lift coefficient whereas the SWB reduces it. Furthermore, while SWB can be turned on or off as required and can thus conserve energy during most phases of a mission profile, the penalty of increased drag and additional deadweight of the canard persists throughout the flight envelope, even when the canard is not needed. The lateral/directional effects of SWB are also much better than effects of the canard (not shown); it enables the airframe to fully exploit its maximum lift without additional stabilizing aids like the wing-leading-edge sawtooth or the mustache on the Kfir-C2 aircraft. The lift curve and drag polar of the close-coupled-canard of Configuration B, with SWB over both wing and canard, are shown in Figs. 21 and 22 for overall comparison. The additional gains in both lift and lift-to-drag ratio are impressive.

4. CONCLUSIONS AND RECOMMENDATIONS

1. Spanwise blowing on Configuration A over the highly swept (60°) delta wing with a conically drooping leading edge increased the maximum lift and the slope of the lift curve. The efficiency of increasing the maximum lift (5.60 for $C_{\mu} = 0.05$ and 4.29 for $C_{\mu} = 0.07$) was higher than previously reported for similar delta wings (Ref. 21) and almost as high as efficiencies found on the moderately swept wings (45° and 32°) of Refs. 8, 19, and 20.
2. SWB over this wing significantly improved the lift-to-drag ratio.
3. Asymmetric blowing did not pose a control problem, but could be used to augment the roll response of the aircraft.
4. The efficiency of the SWB was quadrupled using swirling jets, without any additional penalty. The use of swirling jets has to be further investigated, as well as the possible use of more than one jet to improve mixing and entrainment.
5. SWB increased the lateral/directional stability of Configuration A at low angles of attack and stabilized it in its naturally unstable region of $25^\circ < \alpha < 30^\circ$, thus enabling it to exploit its full maximum-lift capability.
6. SWB over the wing of Configuration A achieved the same lift augmentation (thrust removed) as did the canard, but at a much lower drag.
7. SWB on Configuration B, over the wing only, further improved both the lift curve and the drag polar, but at a lower efficiency than with SWB on Configuration A (without a canard).
8. SWB on both wing and canard of Configuration B augmented the lift and improved the drag polar more than did blowing on the wing alone. The efficiency of SWB over both lifting surfaces was higher than that of blowing over the wing only.
9. In both cases of blowing on Configuration B, the blowing efficiency increased when the jet momentum was increased, contrary to past and present experience with blowing over wings alone.
10. Configuration B was stabilized by SWB up to high yaw angles at angles of attack up to 30° , and could therefore use the maximum lift that could not be reached previously because of lateral/directional instability.
11. SWB on Configuration B has to be investigated in high-subsonic-speed flows where Ref. 20 reported lift augmentation of the order found in the low-speed experiments. Supercritical transonic testing is also needed to find out if the same blowing system, with reasonable momentum coefficients, could achieve the shock-induced-separation control reported in Ref. 24.
12. As a result of Erickson's comments (Ref. 23) about the feasibility of practical application of SWB with engines designed for high bleed rates and low sensitivity of thrust loss to engine bleed, and the success of SWB with the VEO-wing concept, further investigation is recommended concerning the possibility of bleeding the engine combustion products downstream of the turbine instead of bleeding the compressor air. This would require longer and heat-insulated piping but will affect the thrust to a much lesser degree. The hot gases may also be used to preheat the fuel, thus compensating for the remaining thrust loss.

REFERENCES

1. Stanbrook, A. and Squire, L. C., "Possible Types of Flow at Swept Leading Edges," *The Aeronautical Quarterly*, Vol. 15, Feb. 1964, pp. 72-82.
2. Polhamus, E. C., "Predictions of Vortex-Lift Characteristics by a Leading-Edge Suction Analogy," *Journal of Aircraft*, Vol. 8, April 1971, pp. 193-199.
3. Rusak, Z., Wasserstrom, E., and Seginer, A., "Numerical Calculation of Nonlinear Aerodynamics of Wing-Body Configurations," *AIAA Journal*, to be published June or July 1983.

4. Wentz, W. H., Jr. and Kohlman, D. L., "Wind Tunnel Investigations of Vortex Breakdown on Slender Sharp-Edged Wings," NASA CR-98737, 1969.
5. Erickson, G. E., "Effect of Spanwise Blowing on the Aerodynamic Characteristics of a Half-Span 50°-Swept Cropped Delta Wing Configuration," AIAA Paper 79-1859, AIAA Aircraft Systems and Technology Meeting, New York, N.Y., Aug. 1979.
6. Clarke, K. P., "Lift Augmentation on a Moderately Swept Wing by Spanwise Blowing," Aeronautical Journal, Vol. 80, Oct. 1976, pp. 447-451.
7. Kuchemann, D., "On the Possibility of Designing Wings that Combine Vortex Flows with Classical Airfoil Flows," RAE Tech. Memo. Aero. 1363, Oct. 1971.
8. Staudacher, W., Laschka, B., Poisson-Quinton, P., and Ledy, J. P., "Effect of Spanwise Blowing in the Angle-of-Attack Regime $\alpha = 0 \div 90^\circ$," Proceedings of the 11th Congress of ICAS, Vol. 1, Sept. 1978, pp. 85-95.
9. Behrbohn, H., "Basic Low-Speed Aerodynamics of the Short-Coupled Canard Configuration of Small Aspect Ratio," SAAB, Sweden, TN-60, July 1965.
10. Leibovich, S., "The Structure of Vortex Breakdown," Annual Review of Fluid Mechanics, Vol. 10, 1978, pp. 221-246.
11. Cornish, J. J., III, "High Lift Applications of Spanwise Blowing," ICAS Paper No. 70-09, 7th Congress of ICAS, Rome, Italy, Sept. 1970.
12. Dixon, C. J., "The Mechanism of Vortex Control by Spanwise Blowing and Wing Geometry," Lockheed-Georgia Co., Marietta, Ga., Engineering Report LG78-ER-0187, June 1978.
13. Leavitt, D. L., Whitten, P. D., and Stumpfl, S. C., "Low Speed Aerodynamic Characteristics of a Vectored-Engine-Over-Wing Configuration," AIAA Paper 78-1081, AIAA/SAE 14th Joint Propulsion Conference, July 1978.
14. Falarski, M. D., Dudley, M. D., and Howell, G. A., "Analysis of Data from a Wind Tunnel Investigation of a Large-Scale Model of a Highly Maneuverable Supersonic V/STOL Fighter: STOL Configuration," AIAA Paper 81-2620, AIAA/NASA Ames Research Center V/STOL Conference, Dec. 1981.
15. Howell, G. A., "Test Results of Chordwise and Spanwise Blowing for Low-Speed Lift Augmentation," Proceedings of the 13th Congress of ICAS and AIAA Aircraft Systems and Technology Conference, Vol. 2, Aug. 1982, pp. 1222-1234.
16. Dixon, C. J., "Lift Augmentation by Lateral Blowing Over a Lifting Surface," AIAA Paper 69-193, AIAA/AHS VTOL Research, Design and Operations Meeting, Feb. 1969.
17. Poisson-Quinton, P., "Contrôle du D'ecollement D'une Surface Portante par un Jet Transversal," Intervention au 7 iem Congress ICAS, Rome, Sept. 1970.
18. Bradley, R. G. and Wray, W. O., "A Conceptual Study of Leading-Edge-Vortex Enhancement by Blowing," Journal of Aircraft, Vol. 11, Jan. 1974, pp. 33-38.
19. Campbell, J. F., "Augmentation of Vortex Lift by Spanwise Blowing," Journal of Aircraft, Vol. 13, Sept. 1976, pp. 727-732.
20. Bradley, R. G., Whitten, P. D., and Wray, W. O., "Leading-Edge-Vortex Augmentation in Compressible Flow," Journal of Aircraft, Vol. 13, Apr. 1976, pp. 238-242.
21. Anglin, E. L. and Satran, D., "Effects of Spanwise Blowing on Two Fighter Airplane Configurations," AIAA Paper 79-1663, AIAA Atmospheric Flight Mechanics Conference, Aug. 1979.
22. Dixon, C. J., Theisen, J. G., and Scruggs, R. M., "Theoretical and Experimental Investigations of Vortex Lift Control by Spanwise Blowing, Vol. 1, Experimental Research," Lockheed-Georgia Co., Marietta, Ga., Engineering Rept. LG73-ER-0169, Sept. 1973.
23. Erickson, G. E., "Effect of Spanwise Blowing on the Aerodynamic Characteristics of the F-5E," Journal of Aircraft, Vol. 16, Oct. 1979, pp. 695-700.
24. Dixon, C. J., Dansby, T., and Poisson-Quinton, P., "Benefits of Spanwise Blowing at Transonic Speeds," Proceedings of the 11th Congress of ICAS, Vol. 1, Sept. 1978, pp. 72-84.

ACKNOWLEDGMENT

The first author is a National Research Council Research Associate, on leave from the Department of Aeronautical Engineering, Technion-Israel Institute of Technology, Haifa, Israel.

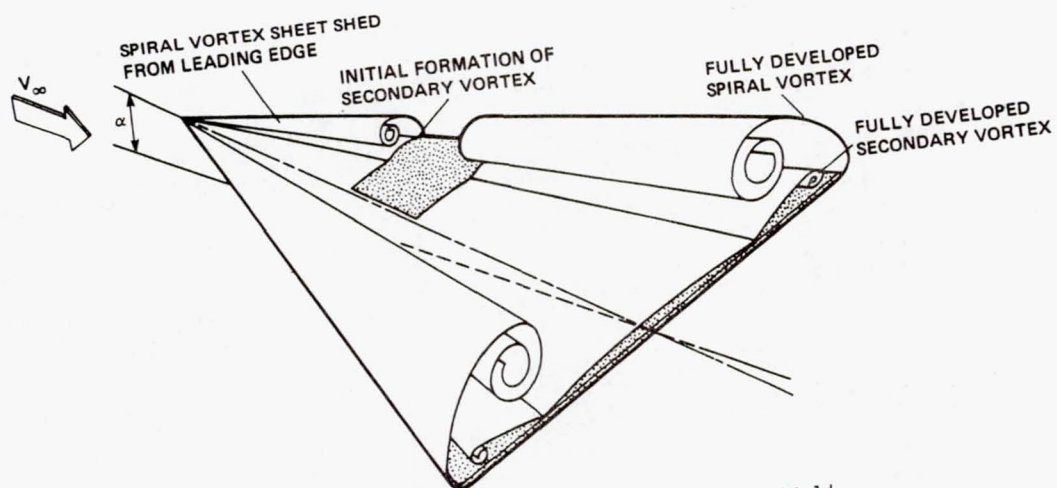


Fig. 1. Sharp leading-edge-induced vortical flow field.

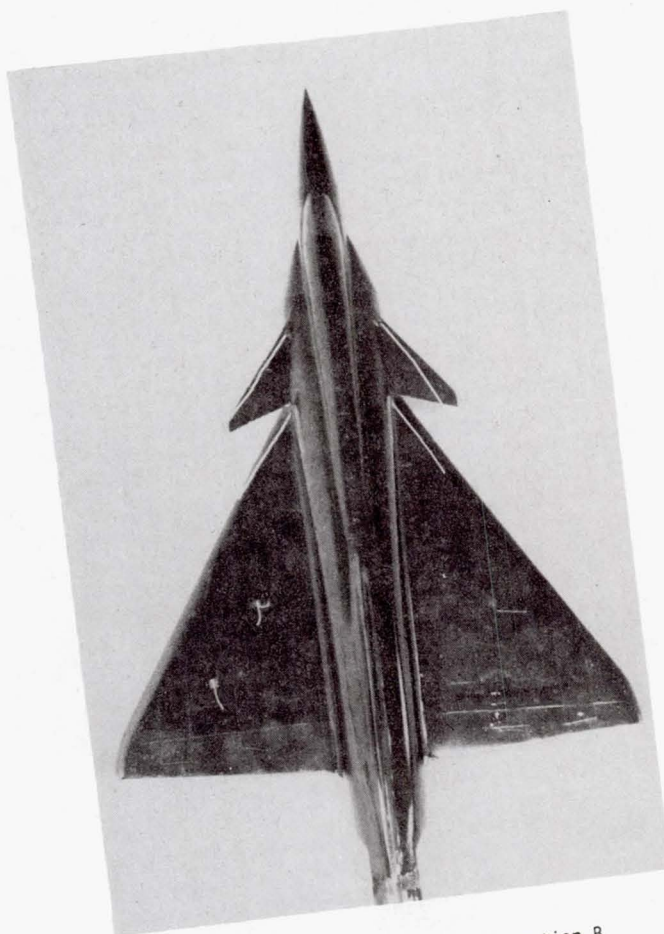


Fig. 2. Aircraft model - Configuration B.

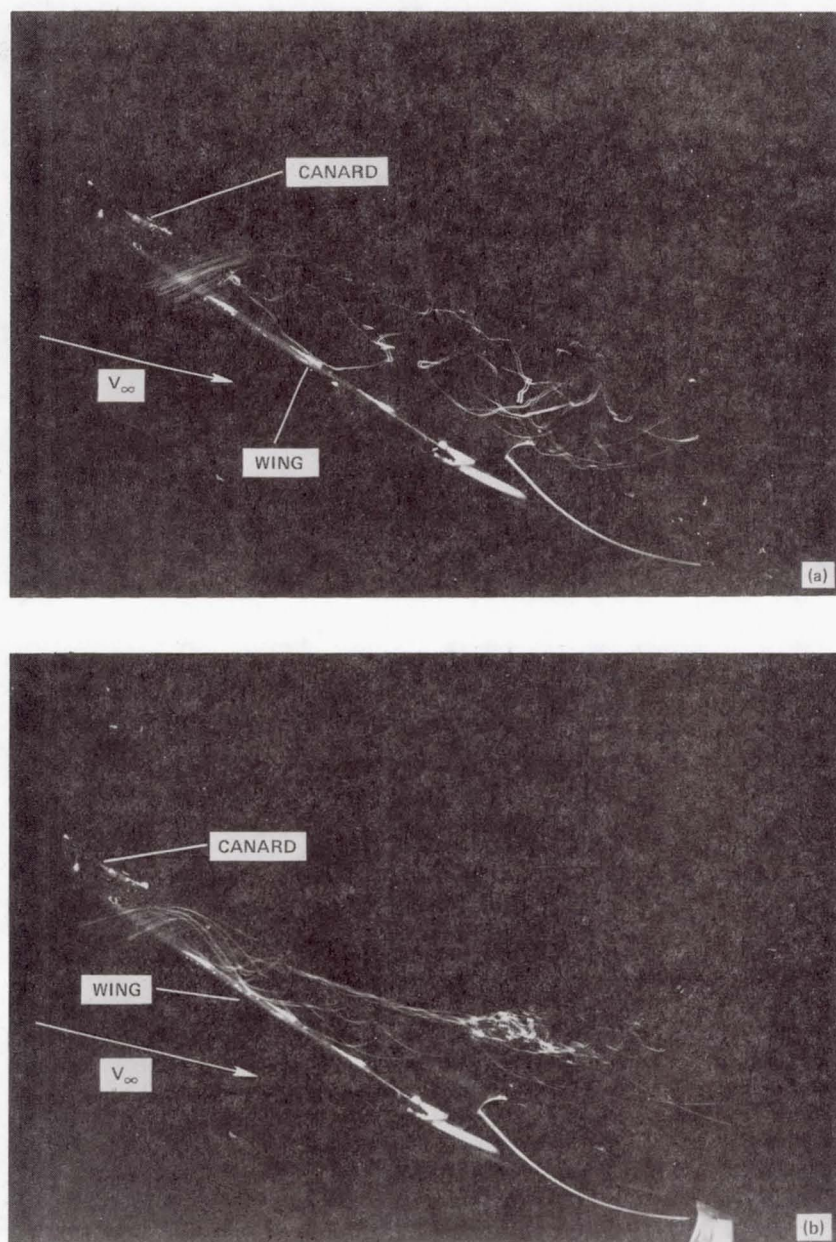


Fig. 3. Main-wing vortex breakdown and stabilization. (a) Breakdown. (b) Stabilization by SWB.

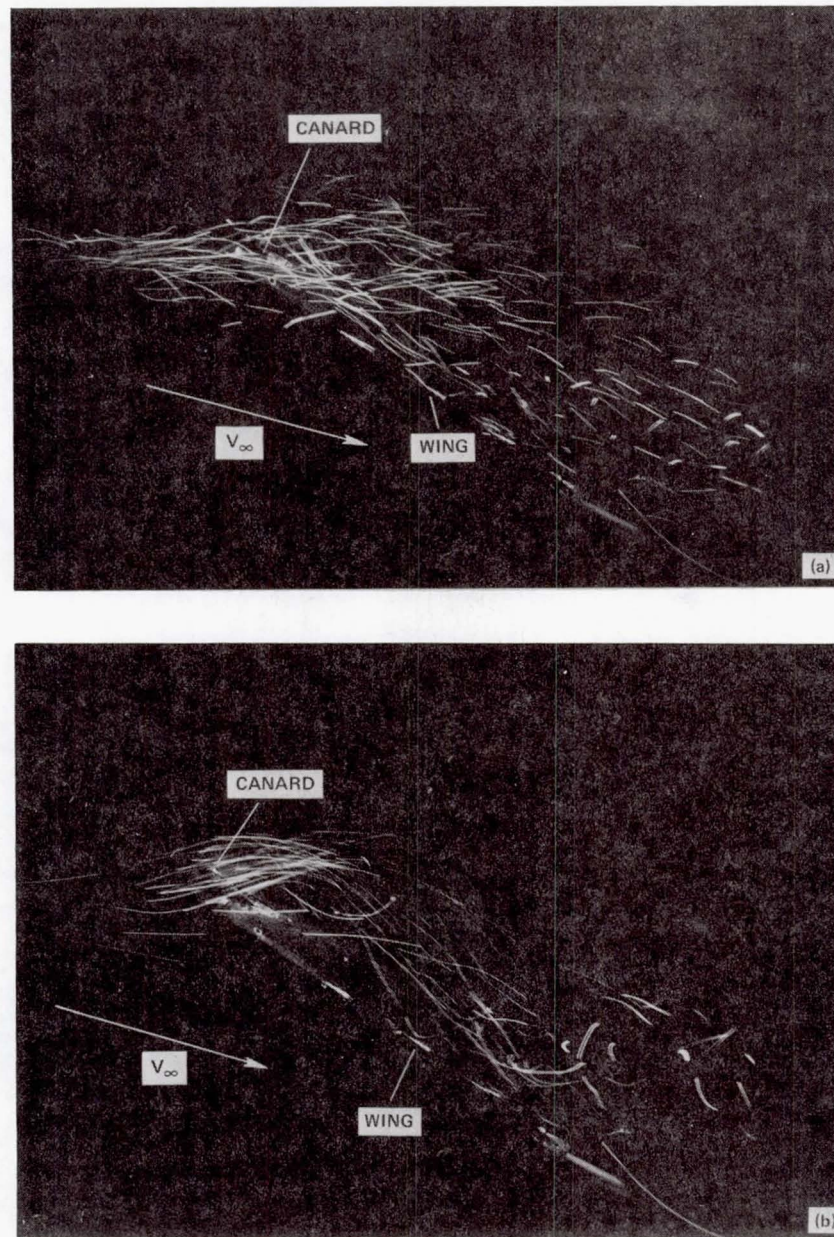


Fig. 4. Canard-vortex breakdown and stabilization. (a) Breakdown. (b) Stabilization by SWB.

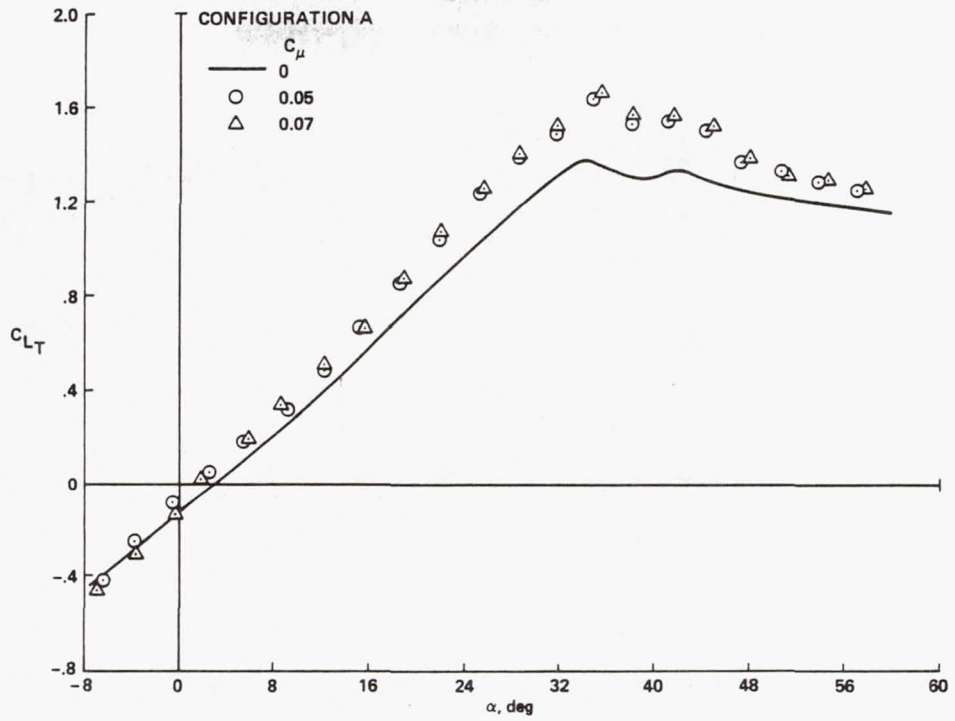


Fig. 5. Configuration A - lift augmentation.

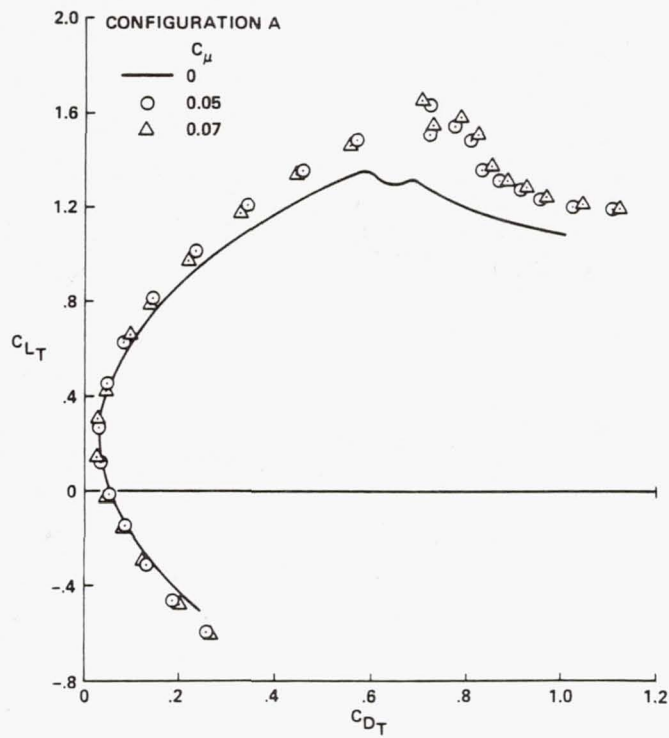


Fig. 6. Configuration A - drag polar.

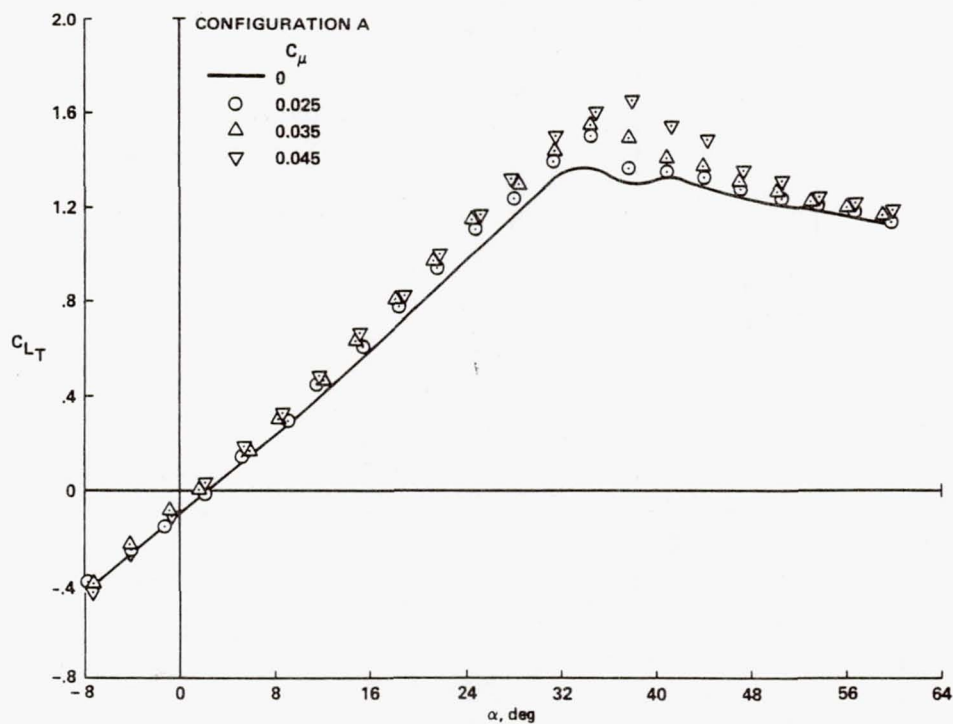


Fig. 7. Lift augmentation - left wing SWB only.

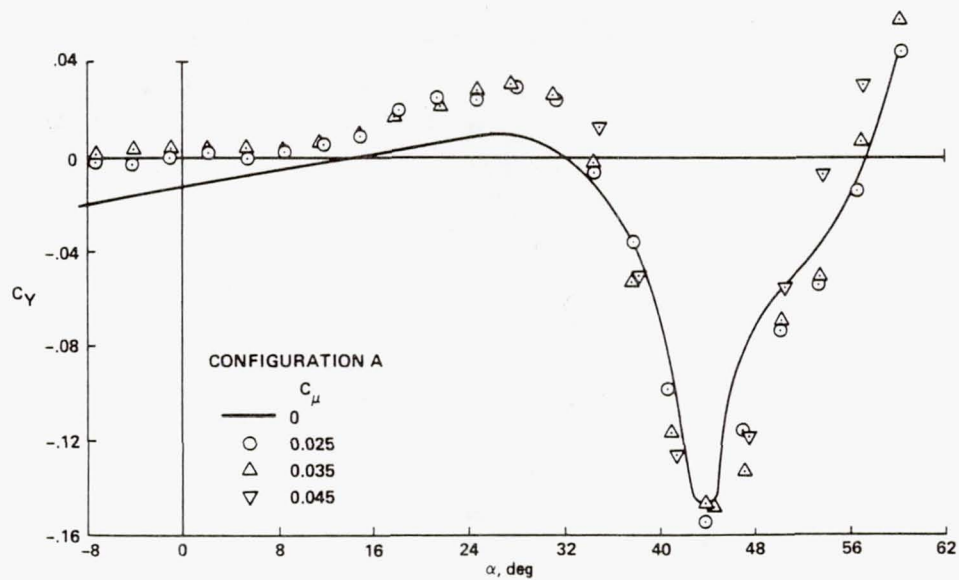


Fig. 8. Side force induced by left wing SWB.

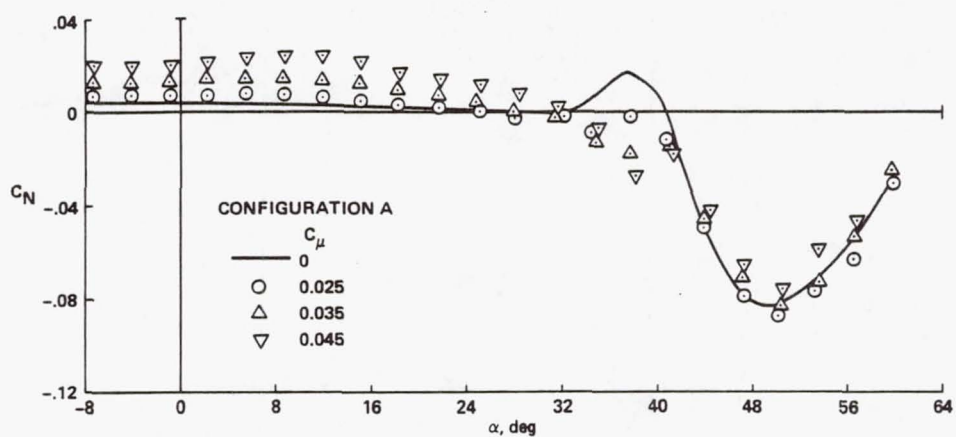


Fig. 9. Yawing moment induced by left wing SWB.

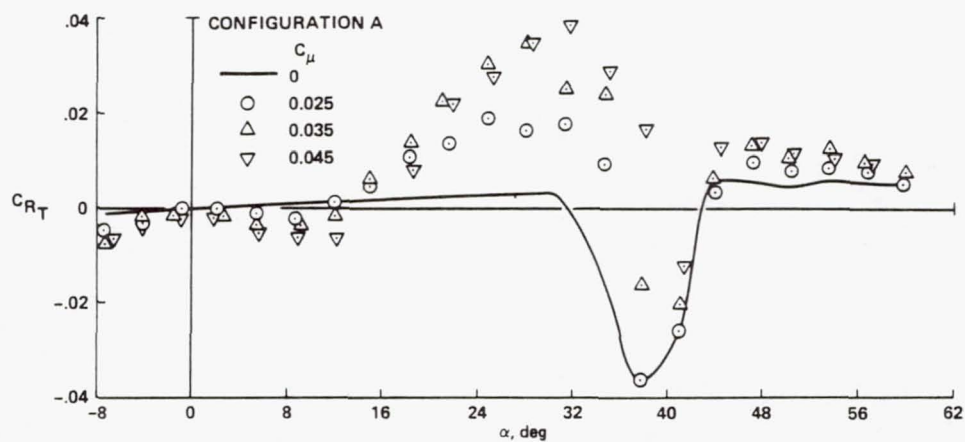


Fig. 10. Rolling moment induced by left wing SWB.

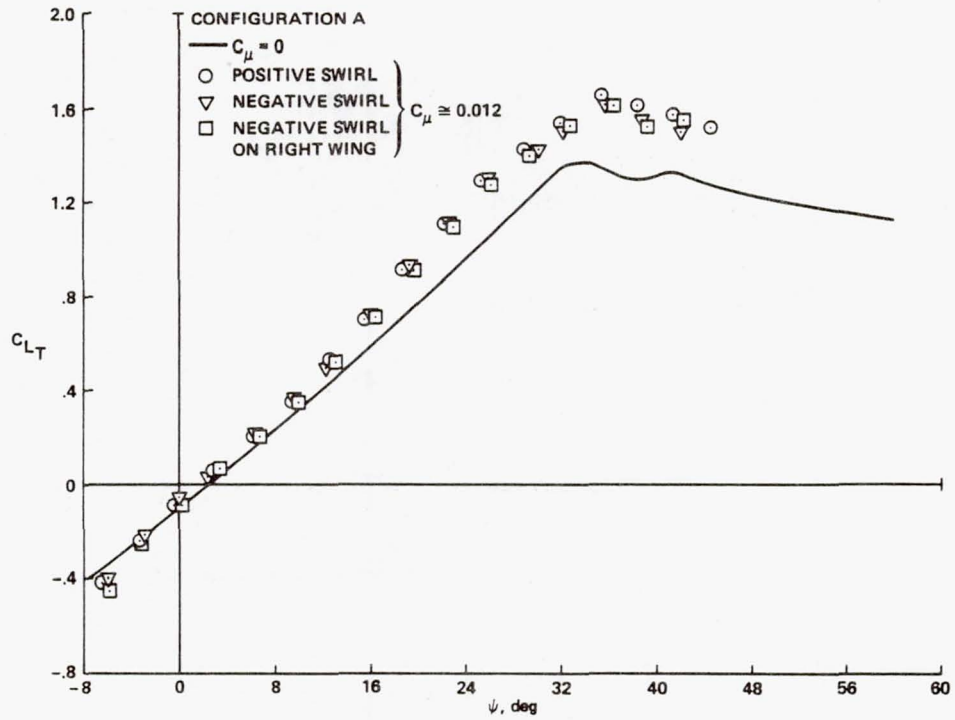


Fig. 11. Lift augmentation - swirling jet SWB.

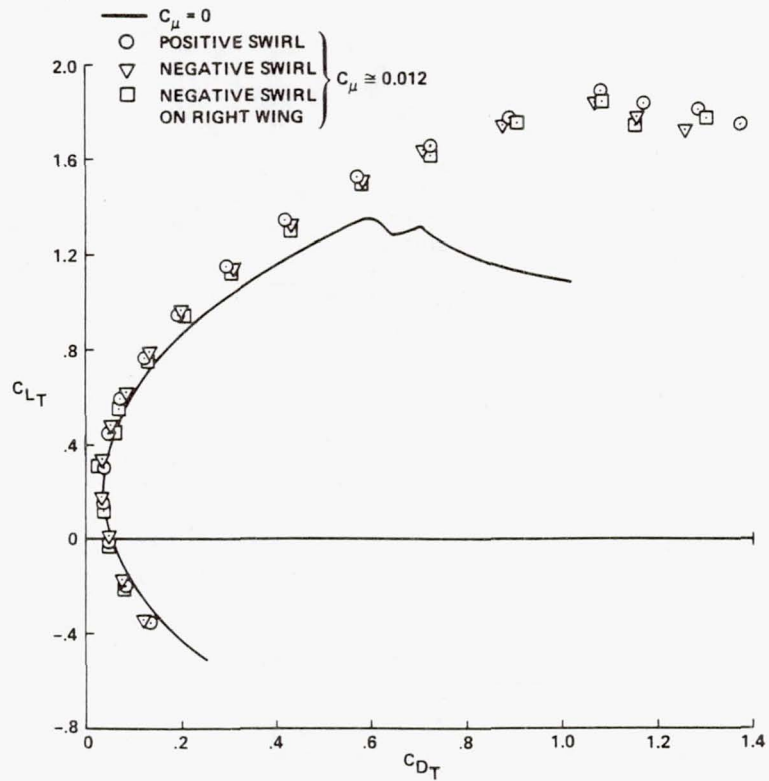


Fig. 12. Drag polar - swirling jet SWB.

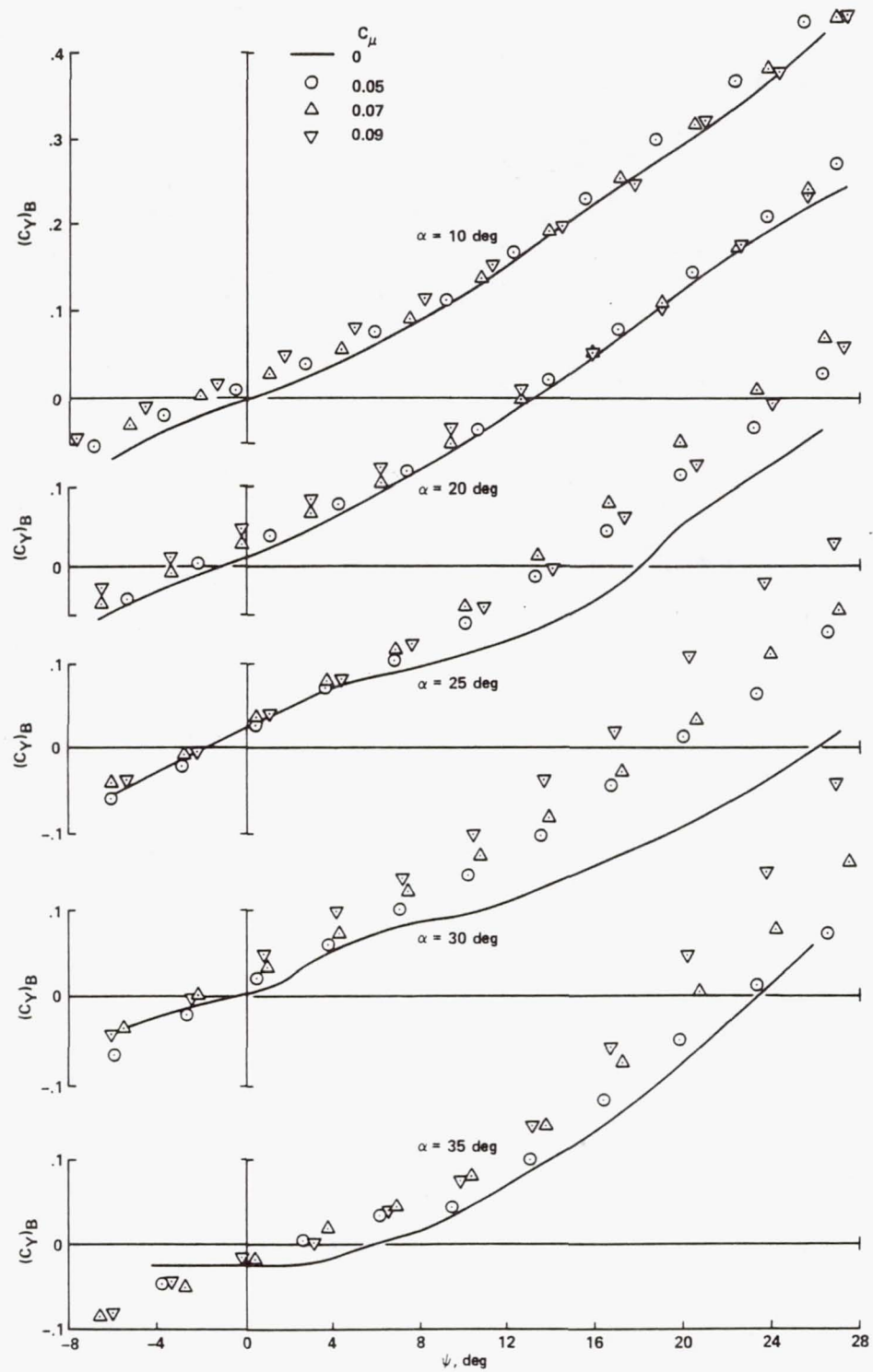
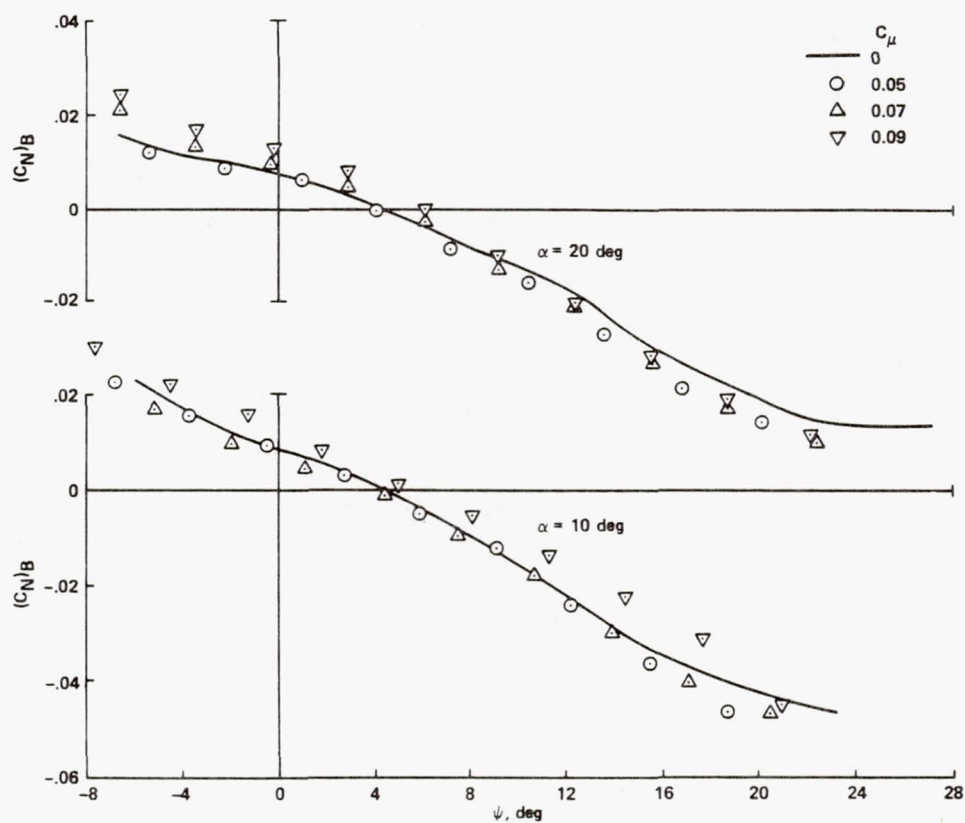
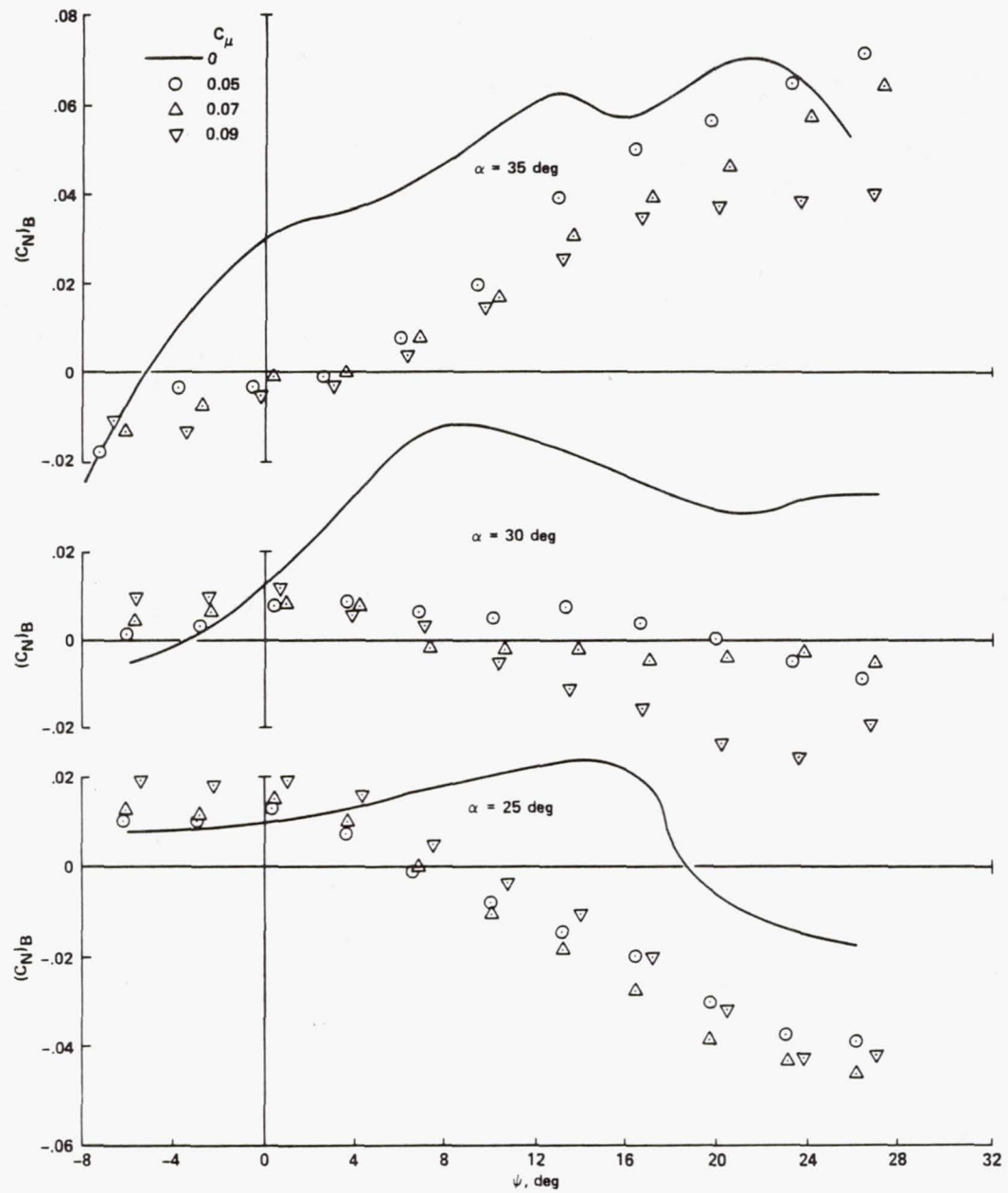


Fig. 13. Configuration A - lateral stability, side forces with SWB.



(a) $\alpha = 10^\circ$ and 20° .

Fig. 14. Configuration A - lateral stability, yawing moments with SWB.



(b) $\alpha = 25^\circ, 30^\circ, \text{ and } 35^\circ$.

Fig. 14. Concluded.

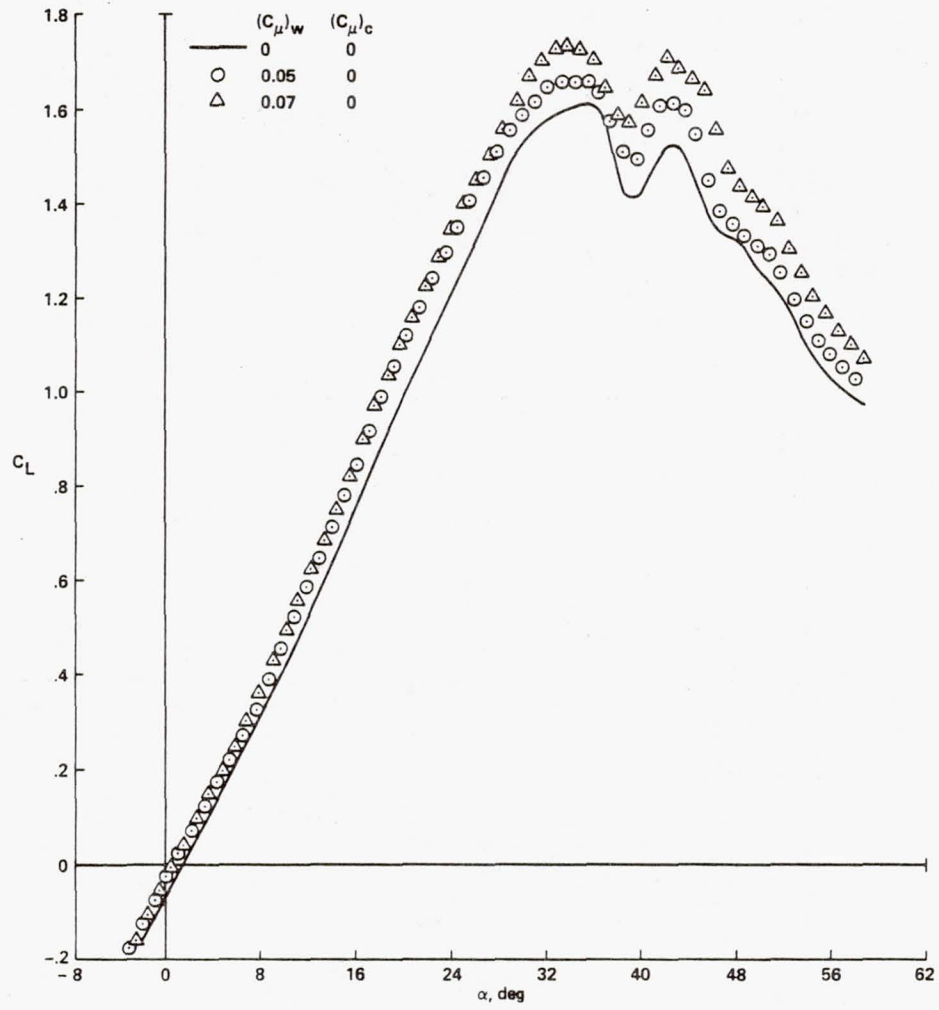


Fig. 15. Configuration B - lift augmentation by SWB over the wing only.

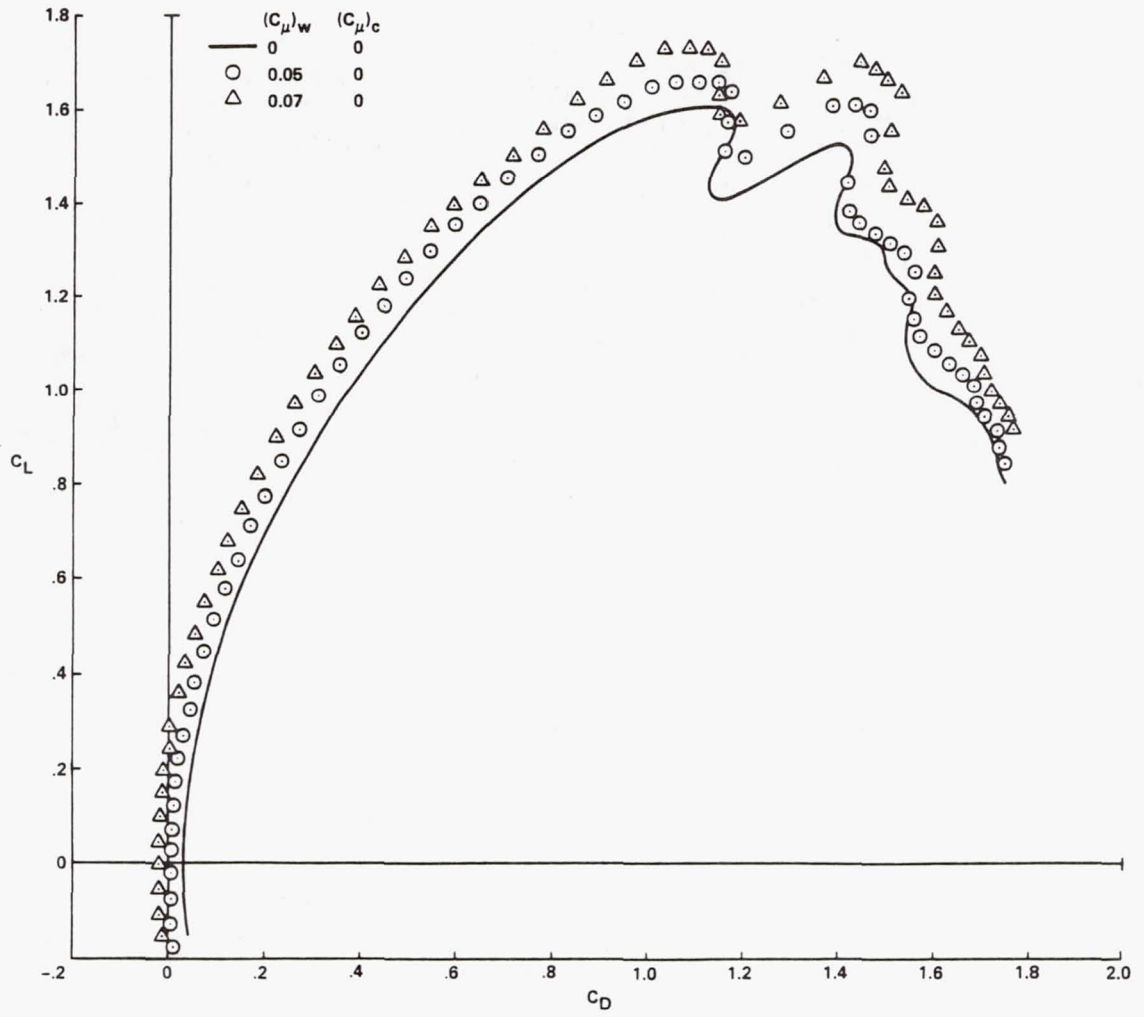


Fig. 16. Configuration B — drag polar by SWB over the wing only.

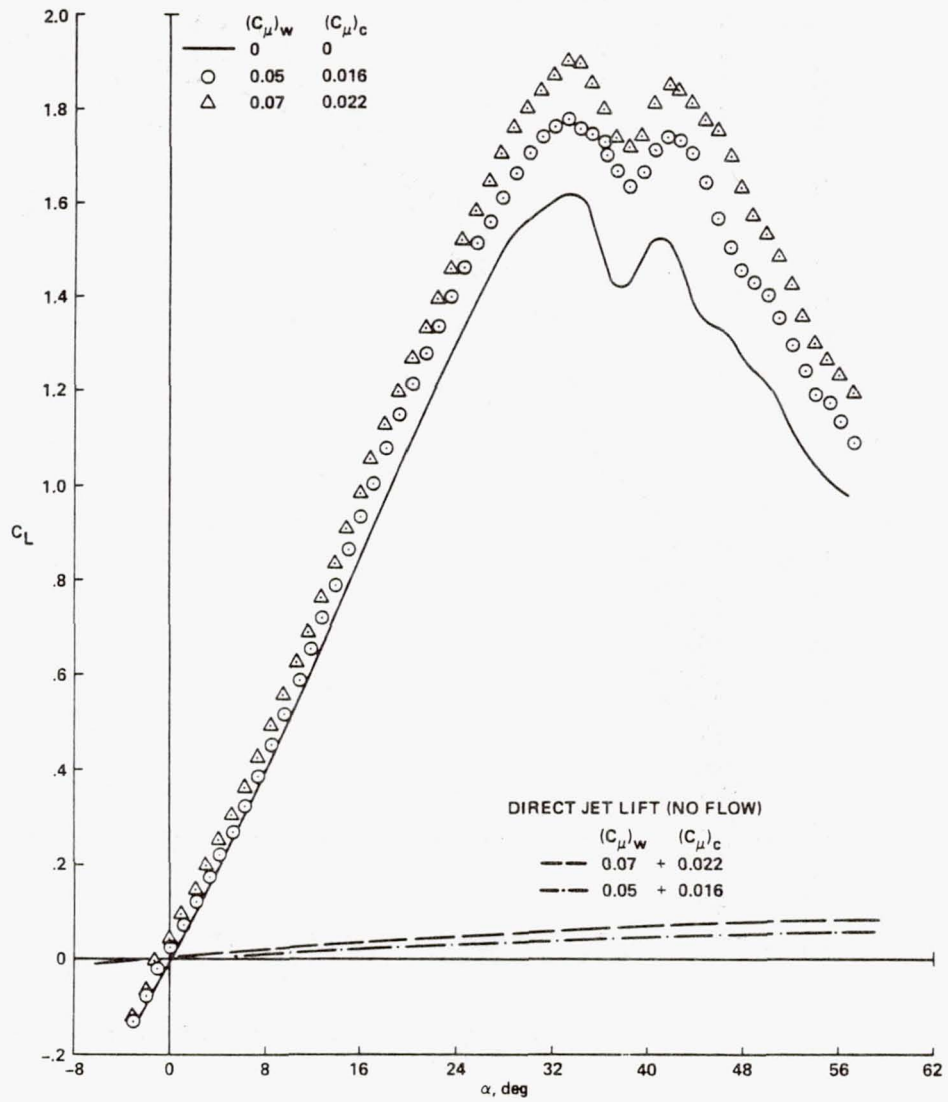


Fig. 17. Configuration B — lift augmentation by SWB over both wing and canard.

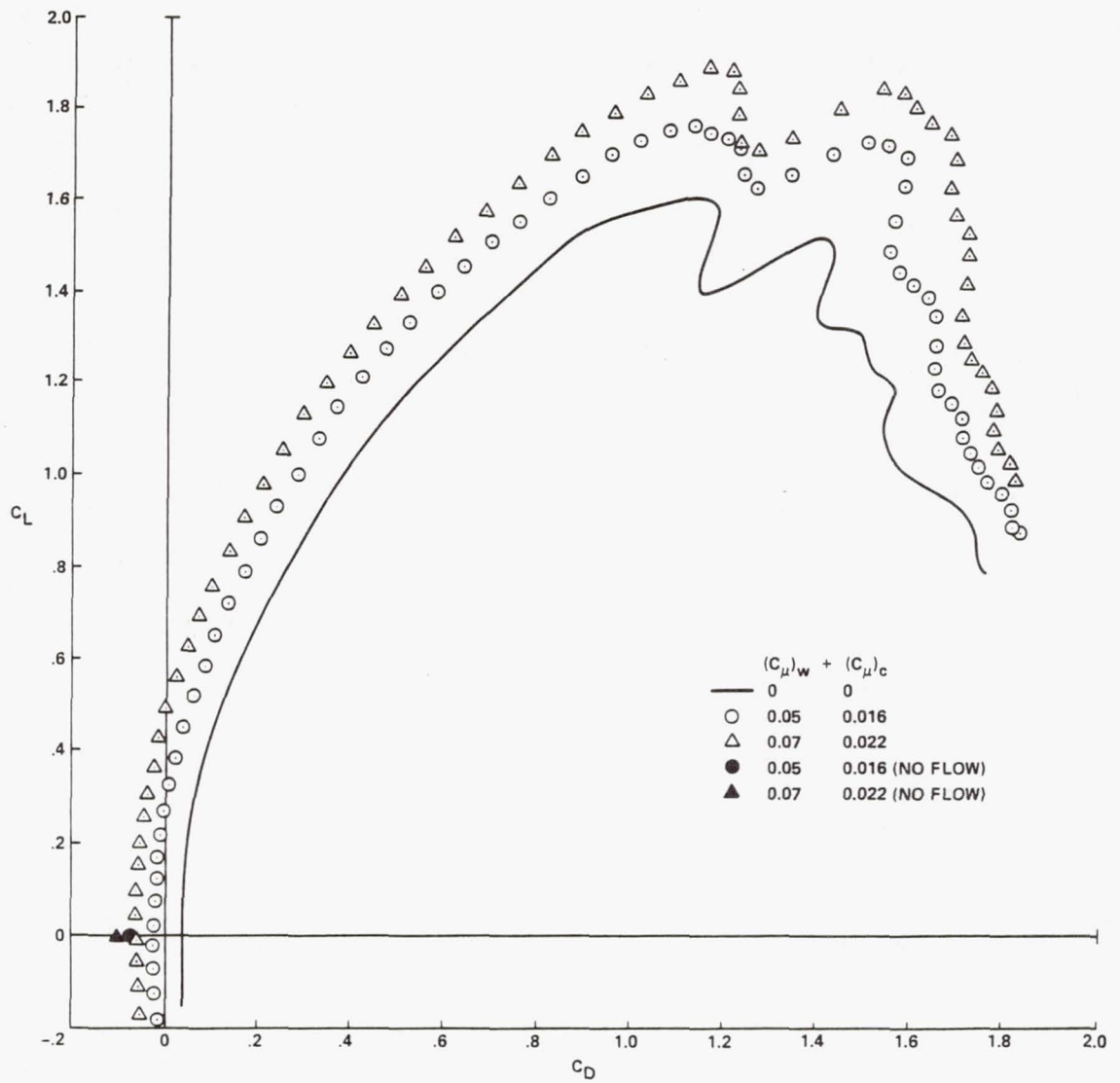


Fig. 18. Configuration B — drag polar by SWB over both wing and canard.

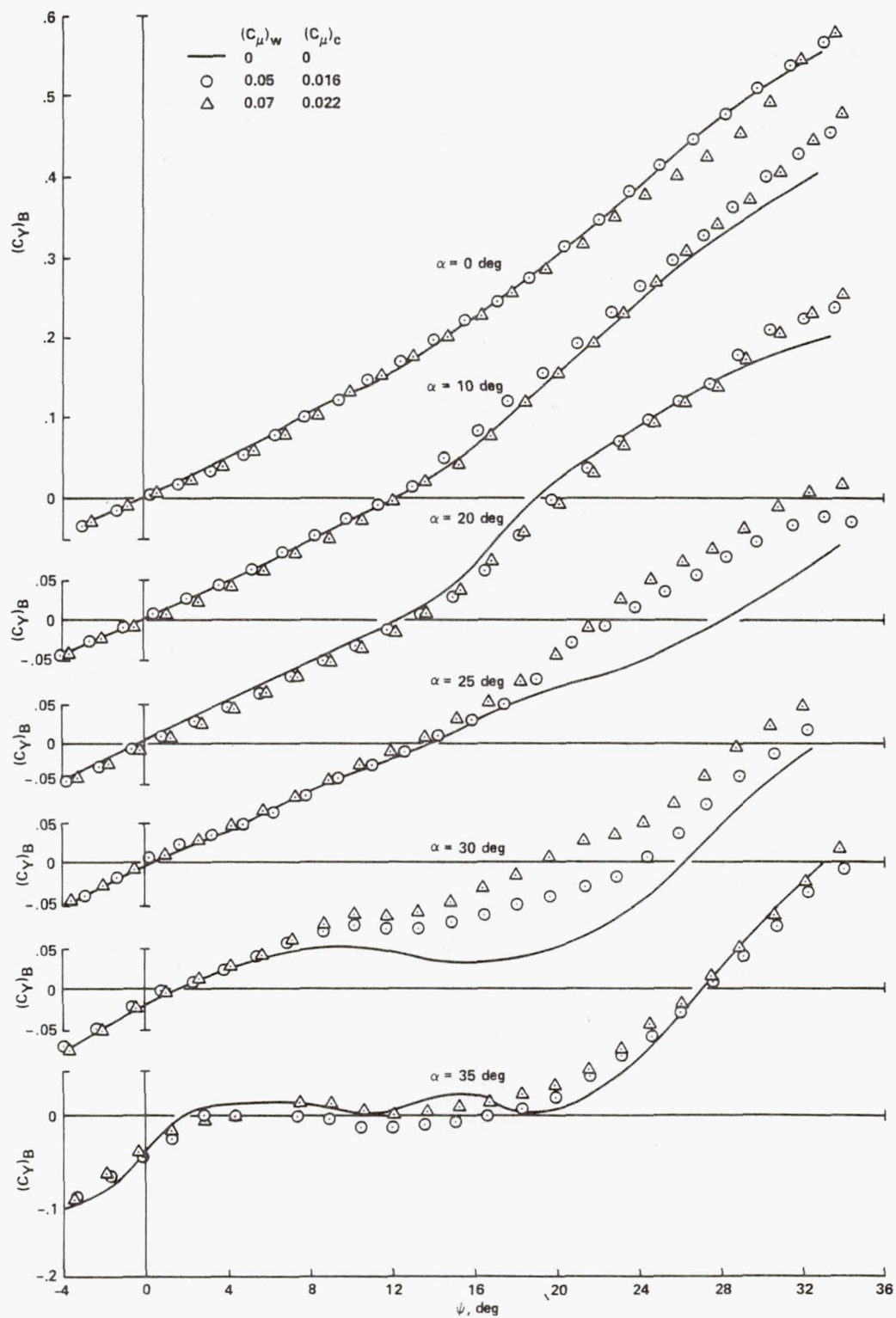
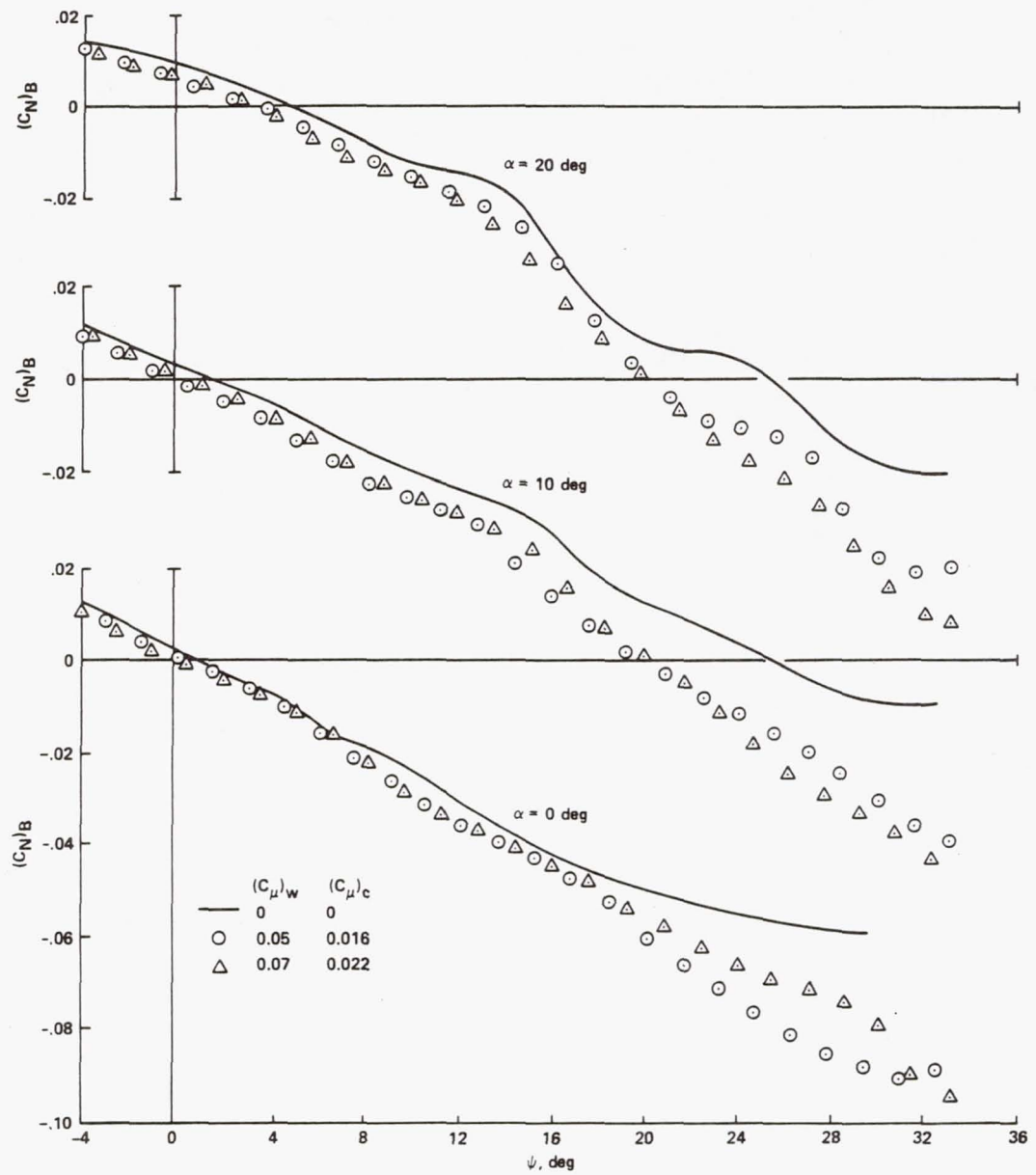
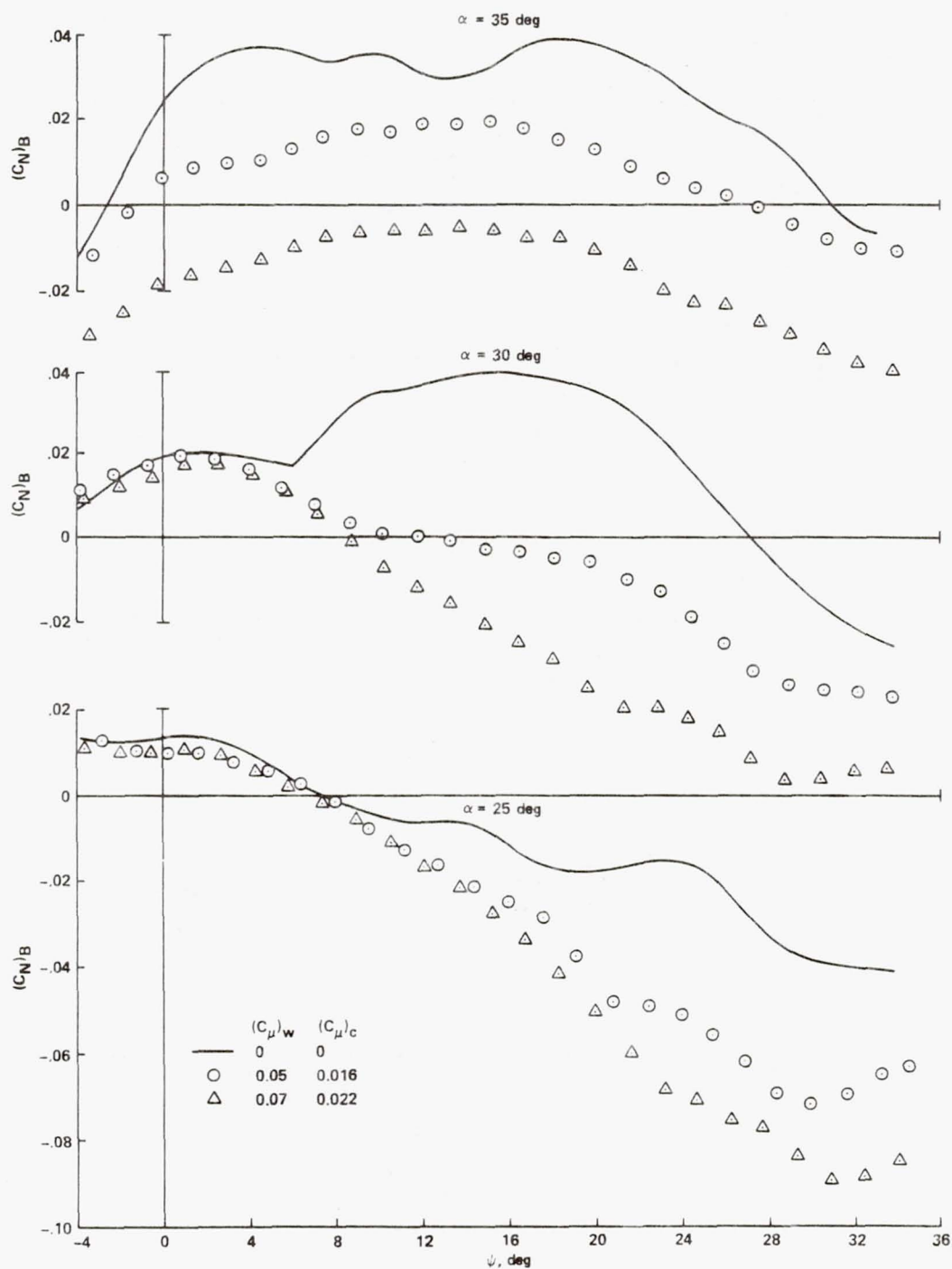


Fig. 19. Configuration B - side forces by SWB over both wing and canard.



(a) $\alpha = 0^\circ, 10^\circ, \text{ and } 20^\circ$.

Fig. 20. Configuration B — yawing moments by SWB over both wing and canard.



(b) $\alpha = 25^\circ, 30^\circ$, and 35° .

Fig. 20. Concluded.

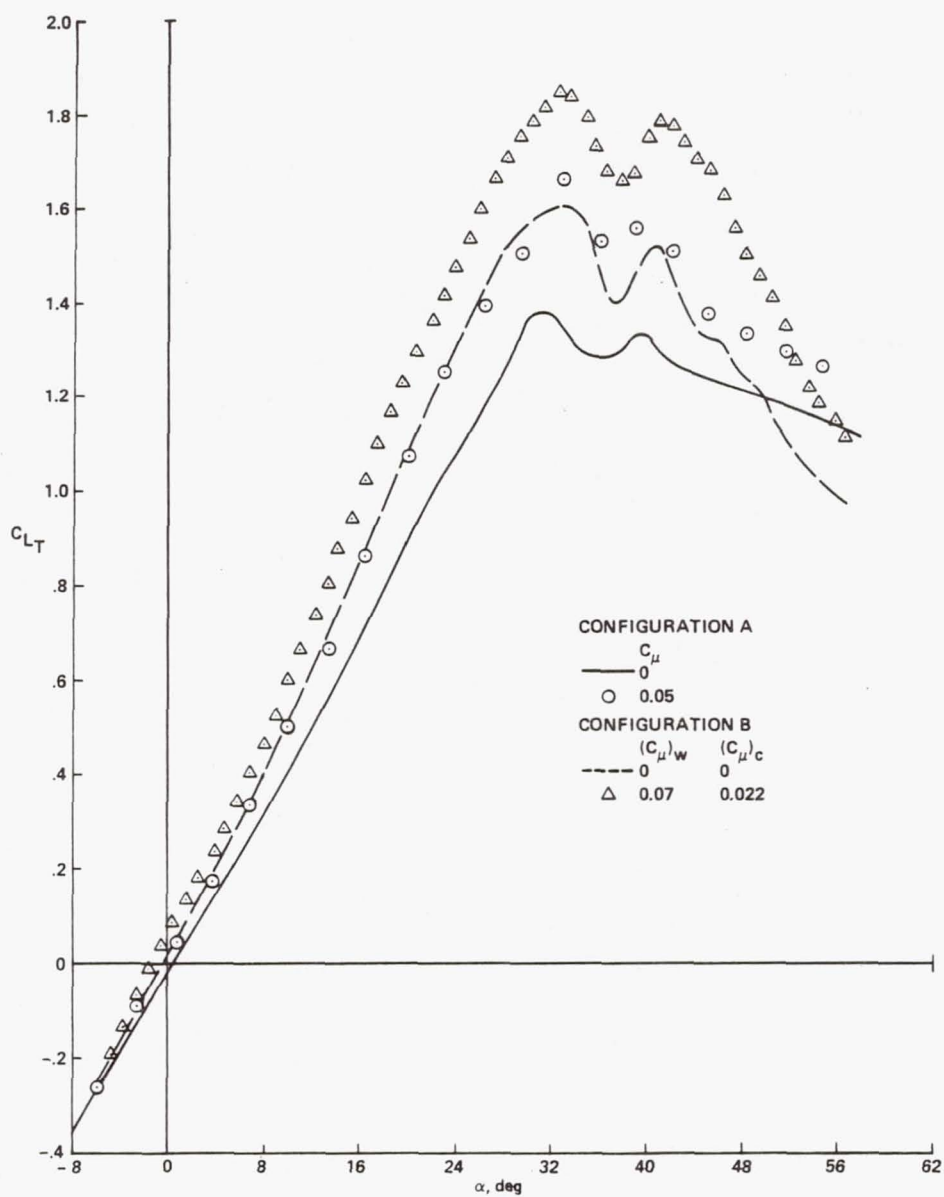


Fig. 21. Lift augmentation - canard versus SWB.

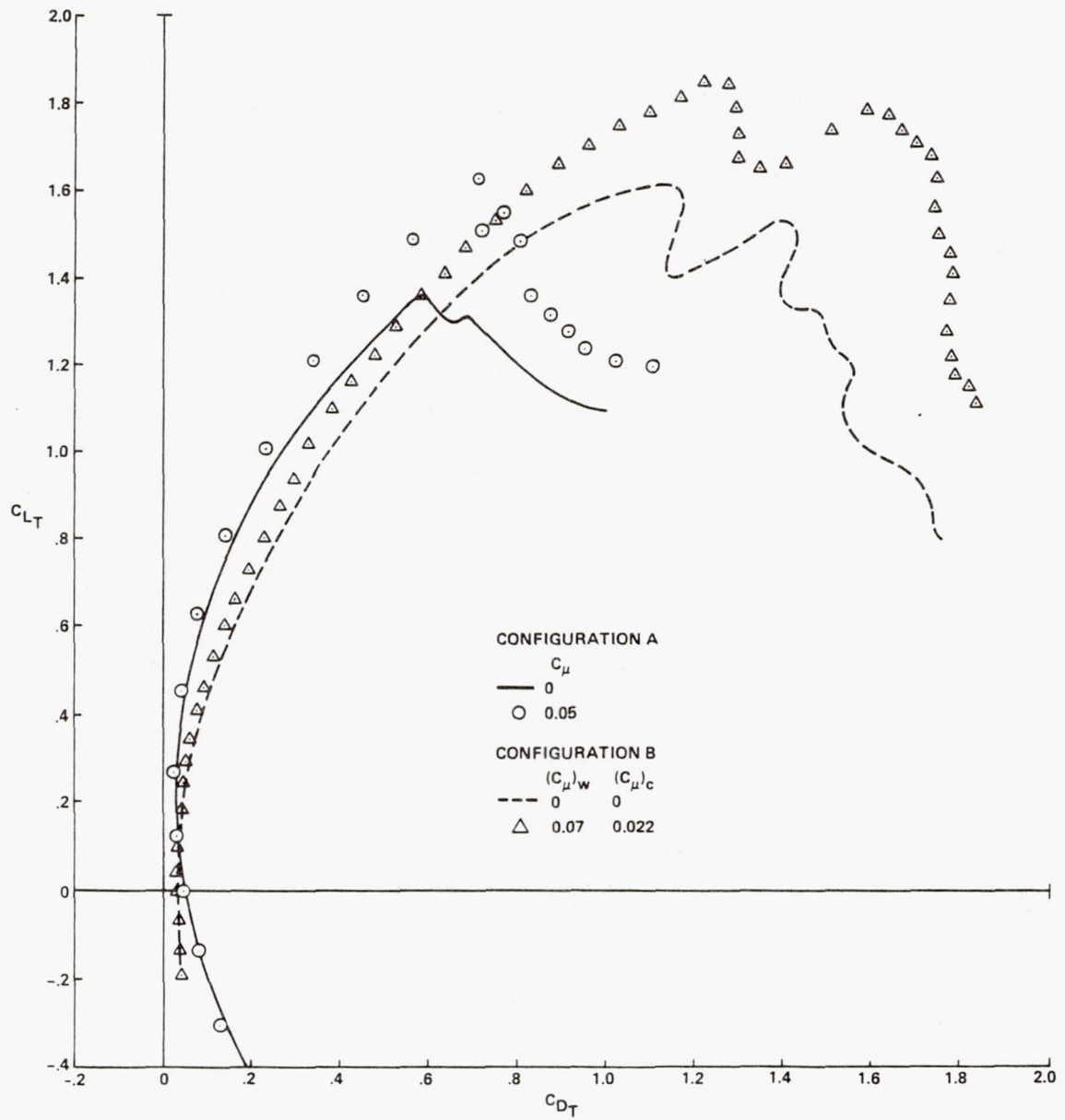


Fig. 22. Drag polar - canard versus SWB.

1. Report No. NASA TM-84330	2. Government Accession No.	3. Recipient's Catalog No.	
4. Title and Subtitle AUGMENTATION OF FIGHTER-AIRCRAFT PERFORMANCE BY SPANWISE BLOWING OVER THE WING LEADING EDGE		5. Report Date March 1983	
		6. Performing Organization Code	
7. Author(s) Arnan Seginer and Meir Salomon*		8. Performing Organization Report No. A-9243	
		10. Work Unit No. T-3414Y	
9. Performing Organization Name and Address NASA Ames Research Center Moffett Field, Calif. 94035		11. Contract or Grant No.	
		13. Type of Report and Period Covered Technical Memorandum	
12. Sponsoring Agency Name and Address National Aeronautics and Space Administration Washington, D.C. 20546		14. Sponsoring Agency Code 505-42-21	
15. Supplementary Notes *SAL Engineering, Haifa, Israel. Point of Contact: Arnan Seginer, Ames Research Center, MS 227-8, Moffett Field, Calif. 94035 (415) 965-5873 or FTS 448-5873.			
16. Abstract Spanwise blowing over the wing and canard of a 1:35 model of a close-coupled-canard fighter-airplane configuration (similar to the Kfir-C2) was investigated experimentally in low-speed flow. Tests were conducted at airspeeds of 30 m/sec (Reynolds number of 1.8×10^5 based on mean aerodynamic chord) with angle-of-attack sweeps from -8° to 60° , and yaw-angle sweeps from -8° to 36° at fixed angles of attack 0° , 10° , 20° , 25° , 30° , and 35° . Significant improvement in lift-curve slope, maximum lift, drag polar and lateral/directional stability was found, enlarging the flight envelope beyond its previous low-speed/maximum-lift limit. In spite of the highly swept (60°) leading edge, the efficiency of the lift augmentation by blowing was relatively high and was found to increase with increasing blowing momentum on the close-coupled-canard configuration. Interesting possibilities of obtaining much higher efficiencies with swirling jets were indicated.			
17. Key Words (Suggested by Author(s)) Spanwise blowing Vortex lift Aircraft performance		18. Distribution Statement Unlimited Subject Category - 02	
19. Security Classif. (of this report) Unclassified	20. Security Classif. (of this page) Unclassified	21. No. of Pages 29	22. Price* A03